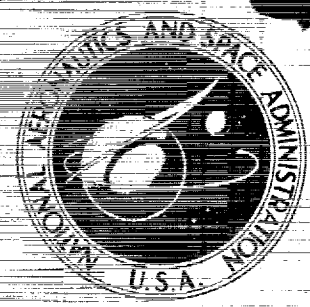


467-15816

[REDACTED]

NASA CONTRACTOR REPORT



UB
NASA CR-697

N70-72931

CASE FILE
COPY

CLASSIFICATION CHANGED
UNCLASSIFIED

By Authority of *LIA/D 70-37* Date *2-20-69*

[REDACTED]

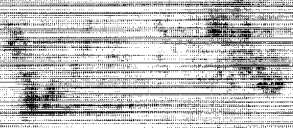
NUCLEAR CRITICALITY STUDY OF A SPECIFIC VORTEX-STABILIZED GASEOUS NUCLEAR ROCKET ENGINE

by *T. S. Latham*

Declassified by authority of NASA
Classification Change Notice No. *193*
Dated *28 FEB 1970*

Prepared by
UNITED AIRCRAFT CORPORATION
Hartford, Conn.

[REDACTED]



NUCLEAR CRITICALITY STUDY OF A SPECIFIC VORTEX-STABILIZED
GASEOUS NUCLEAR ROCKET ENGINE

By T. S. Latham

Distribution of this report is provided in the interest of
information exchange. Responsibility for the contents
resides in the author or organization that prepared it.

GROUP 4
Downgraded at 3 year intervals;
declassified after 12 years

Prepared under Contract No. NASw-847 by
UNITED AIRCRAFT CORPORATION
East Hartford, Conn.

for

NATIONAL AERONAUTICS AND SPACE ADMINISTRATION

1 2 3 4 5 6 7 8 9 10 11 12 13 14 15 16 17 18 19 20 21 22 23 24 25 26 27 28 29 30 31 32 33 34 35 36 37 38 39 40 41 42 43 44 45 46 47 48 49 50 51 52 53 54 55 56 57 58 59 60 61 62 63 64 65 66 67 68 69 70 71 72 73 74 75 76 77 78 79 80 81 82 83 84 85 86 87 88 89 90 91 92 93 94 95 96 97 98 99 100

1 2 3 4 5 6 7 8 9 10 11 12 13 14 15 16 17 18 19 20 21 22 23 24 25 26 27 28 29 30 31 32 33 34 35 36 37 38 39 40 41 42 43 44 45 46 47 48 49 50 51 52 53 54 55 56 57 58 59 60 61 62 63 64 65 66 67 68 69 70 71 72 73 74 75 76 77 78 79 80 81 82 83 84 85 86 87 88 89 90 91 92 93 94 95 96 97 98 99 100

1 2 3 4 5 6 7 8 9 10 11 12 13 14 15 16 17 18 19 20 21 22 23 24 25 26 27 28 29 30 31 32 33 34 35 36 37 38 39 40 41 42 43 44 45 46 47 48 49 50 51 52 53 54 55 56 57 58 59 60 61 62 63 64 65 66 67 68 69 70 71 72 73 74 75 76 77 78 79 80 81 82 83 84 85 86 87 88 89 90 91 92 93 94 95 96 97 98 99 100

1 2 3 4 5 6 7 8 9 10 11 12 13 14 15 16 17 18 19 20 21 22 23 24 25 26 27 28 29 30 31 32 33 34 35 36 37 38 39 40 41 42 43 44 45 46 47 48 49 50 51 52 53 54 55 56 57 58 59 60 61 62 63 64 65 66 67 68 69 70 71 72 73 74 75 76 77 78 79 80 81 82 83 84 85 86 87 88 89 90 91 92 93 94 95 96 97 98 99 100

1 2 3 4 5 6 7 8 9 10 11 12 13 14 15 16 17 18 19 20 21 22 23 24 25 26 27 28 29 30 31 32 33 34 35 36 37 38 39 40 41 42 43 44 45 46 47 48 49 50 51 52 53 54 55 56 57 58 59 60 61 62 63 64 65 66 67 68 69 70 71 72 73 74 75 76 77 78 79 80 81 82 83 84 85 86 87 88 89 90 91 92 93 94 95 96 97 98 99 100

SECRET

FOREWORD

An exploratory experimental and theoretical investigation of gaseous nuclear rocket technology is being conducted by the United Aircraft Corporation Research Laboratories under Contract NASw-847 with the joint AEC-NASA Space Nuclear Propulsion Office. The Technical Supervisor of the Contract for NASA is Captain W. A. Yingling (USAF). Results of the investigation conducted during the period between September 15, 1965 and September 15, 1966 are described in the following six reports (including the present report) which comprise the required fourth Interim Summary Technical Report under the Contract:

1. Krascella, N. L.: Theoretical Investigation of the Absorptive Properties of Small Particles and Heavy-Atom Gases. NASA CR-693, 1967. (Unclassified)
2. Kinney, R. B.: Theoretical Effect of Seed Opacity and Turbulence on Temperature Distributions in the Propellant Region of a Vortex-Stabilized Gaseous Nuclear Rocket (U). NASA CR-694, 1967. (Report classified Confidential)
3. Kesten, A. S., and N. L. Krascella: Theoretical Investigation of Radiant Heat Transfer in the Fuel Region of a Gaseous Nuclear Rocket Engine. NASA CR-695, 1967. (Unclassified)
4. Roback, R.: Theoretical Performance of Rocket Engines Using Gaseous Hydrogen in the Ideal State at Stagnation Temperatures up to 20,000 R. NASA CR-696, 1967. (Unclassified)
5. Latham, T. S.: Nuclear Criticality Study of a Specific Vortex-Stabilized Gaseous Nuclear Rocket Engine (U). NASA CR-697, 1967. (Report classified Confidential) (present report)
6. McLafferty, G. H., H. E. Bauer, and D. E. Sheldon: Preliminary Conceptual Design Study of a Specific Vortex-Stabilized Gaseous Nuclear Rocket Engine (U). NASA CR-698, 1967. (Report classified Confidential)

1
 2
 3
 4
 5
 6
 7
 8
 9
 10
 11
 12
 13
 14
 15
 16
 17
 18
 19
 20
 21
 22
 23
 24
 25
 26
 27
 28
 29
 30
 31
 32
 33
 34
 35
 36
 37
 38
 39
 40
 41
 42
 43
 44
 45
 46
 47
 48
 49
 50
 51
 52
 53
 54
 55
 56
 57
 58
 59
 60
 61
 62
 63
 64
 65
 66
 67
 68
 69
 70
 71
 72
 73
 74
 75
 76
 77
 78
 79
 80
 81
 82
 83
 84
 85
 86
 87
 88
 89
 90
 91
 92
 93
 94
 95
 96
 97
 98
 99
 100
 101
 102
 103
 104
 105
 106
 107
 108
 109
 110
 111
 112
 113
 114
 115
 116
 117
 118
 119
 120
 121
 122
 123
 124
 125
 126
 127
 128
 129
 130
 131
 132
 133
 134
 135
 136
 137
 138
 139
 140
 141
 142
 143
 144
 145
 146
 147
 148
 149
 150
 151
 152
 153
 154
 155
 156
 157
 158
 159
 160
 161
 162
 163
 164
 165
 166
 167
 168
 169
 170
 171
 172
 173
 174
 175
 176
 177
 178
 179
 180
 181
 182
 183
 184
 185
 186
 187
 188
 189
 190
 191
 192
 193
 194
 195
 196
 197
 198
 199
 200
 201
 202
 203
 204
 205
 206
 207
 208
 209
 210
 211
 212
 213
 214
 215
 216
 217
 218
 219
 220
 221
 222
 223
 224
 225
 226
 227
 228
 229
 230
 231
 232
 233
 234
 235
 236
 237
 238
 239
 240
 241
 242
 243
 244
 245
 246
 247
 248
 249
 250
 251
 252
 253
 254
 255
 256
 257
 258
 259
 260
 261
 262
 263
 264
 265
 266
 267
 268
 269
 270
 271
 272
 273
 274
 275
 276
 277
 278
 279
 280
 281
 282
 283
 284
 285
 286
 287
 288
 289
 290
 291
 292
 293
 294
 295
 296
 297
 298
 299
 300
 301
 302
 303
 304
 305
 306
 307
 308
 309
 310
 311
 312
 313
 314
 315
 316
 317
 318
 319
 320
 321
 322
 323
 324
 325
 326
 327
 328
 329
 330
 331
 332
 333
 334
 335
 336
 337
 338
 339
 340
 341
 342
 343
 344
 345
 346
 347
 348
 349
 350
 351
 352
 353
 354
 355
 356
 357
 358
 359
 360
 361
 362
 363
 364
 365
 366
 367
 368
 369
 370
 371
 372
 373
 374
 375
 376
 377
 378
 379
 380
 381
 382
 383
 384
 385
 386
 387
 388
 389
 390
 391
 392
 393
 394
 395
 396
 397
 398
 399
 400
 401
 402
 403
 404
 405
 406
 407
 408
 409
 410
 411
 412
 413
 414
 415
 416
 417
 418
 419
 420
 421
 422
 423
 424
 425
 426
 427
 428
 429
 430
 431
 432
 433
 434
 435
 436
 437
 438
 439
 440
 441
 442
 443
 444
 445
 446
 447
 448
 449
 450
 451
 452
 453
 454
 455
 456
 457
 458
 459
 460
 461
 462
 463
 464
 465
 466
 467
 468
 469
 470
 471
 472
 473
 474
 475
 476
 477
 478
 479
 480
 481
 482
 483
 484
 485
 486
 487
 488
 489
 490
 491
 492
 493
 494
 495
 496
 497
 498
 499
 500
 501
 502
 503
 504
 505
 506
 507
 508
 509
 510
 511
 512
 513
 514
 515
 516
 517
 518
 519
 520
 521
 522
 523
 524
 525

Nuclear Criticality Study of a Specific Vortex-
Stabilized Gaseous Nuclear Rocket Engine

TABLE OF CONTENTS

	<u>Page</u>
SUMMARY.....	1
RESULTS.....	2
INTRODUCTION.....	3
STEPS IN NUCLEAR ANALYSIS.....	4
ENGINE SPECIFICATIONS AND NUCLEAR CONFIGURATIONS.....	5
NEUTRON CROSS SECTIONS.....	9
Treatment of Hot Hydrogen Scattering.....	10
Comparison of 24-Group and 4-Group Cross Sections.....	11
RESULTS OF ONE-DIMENSIONAL DIFFUSION THEORY CALCULATIONS	
24-Group Calculations.....	12
14-Group Calculations.....	13
RESULTS OF TWO-DIMENSIONAL DIFFUSION THEORY CALCULATIONS.....	17
REFERENCES.....	21
LIST OF SYMBOLS.....	24
TABLES.....	26
FIGURES.....	42

[illegible]

[REDACTED]

[REDACTED]

Nuclear Criticality Study of a Specific Vortex-
Stabilized Gaseous Nuclear Rocket Engine

SUMMARY

An analytical study was conducted using one- and two-dimensional diffusion theory to determine the critical mass requirements of a specific reference vortex-stabilized gaseous nuclear rocket engine configuration having a cavity length and diameter equal to 6 ft, a cavity liner composed of tubes made from W-184, and a surrounding moderator region made of successive layers of beryllium, beryllium oxide, graphite, and heavy water. The calculations made allowance for the following: an annular passage leading from the cavity to the exhaust nozzles, a fuel-injection duct passing through the moderator, voids and W-184 structure in the moderator, a radial distribution of hydrogen temperature in the cavity, and a radial fuel density distribution. In addition, the moderator was considered to be surrounded by layers of natural tungsten and iron to simulate the external piping and pressure vessel.

The results of the calculations indicate that a critical mass of 50.1 lb of U-233 fuel would be required for the reference engine design used in the present study. This mass could be reduced by a decrease in the volume of the nozzle-approach annulus, an increase in reflector-moderator mass, or a reduction in the volume of neutron-absorbing structure within the cavity liner and reflector-moderator. For instance, one-dimensional calculations indicate that the critical mass could be reduced by approximately 40% by substitution of beryllium wall liner tubes covered with niobium-carbide-coated graphite sleeves for the W-184 wall liner tubes assumed in the study.

One-dimensional calculations were performed to generate 4-group cross sections for subsequent two-dimensional calculations and also to provide information on trends in critical mass variation with variations in moderator void fractions, structure fractions, dimension of various regions, and selection of nuclear fuel. The two-dimensional calculations provide critical mass estimates for configurations with and without exhaust nozzles and fuel-injection duct, and with different amounts of structure within the exhaust nozzle region.

RESULTS

1. A critical mass of 50.1 lb of U-233 was determined for the specific reference engine design considered in the study on the basis of two-dimensional calculations.
2. The critical mass of the reference engine design would be reduced by approximately 40% by elimination of W-184 from the cavity surface liner and moderator regions on the basis of one-dimensional calculations.
3. Replacement of U-233 with U-235 or Pu-239 in the reference engine design would result in an increase in critical mass by factors of 3.25 and 4.05, respectively, on the basis of one-dimensional calculations.
4. A decrease in fuel radius and an increase in thickness of the cold hydrogen layer near the cavity wall have compensating effects on required critical mass, an important result when considering the stability of the radius of the fuel region. For the reference engine, a decrease in fuel radius of one centimeter results in an increase in critical mass of 0.5%, while an increase in the thickness of the cool hydrogen layer of one centimeter results in a decrease in critical mass of 2.8% on the basis of one-dimensional calculations.
5. Elimination of the exhaust nozzle approach annulus from the reference engine design would reduce the critical mass by approximately 20% on the basis of two-dimensional calculations. Although the exhaust nozzle approach annulus cannot be completely eliminated, its volume can be reduced with an accompanying reduction in critical mass.
6. Elimination of the fuel injection duct from the reference engine design would reduce critical mass by approximately 8% on the basis of simplified one-dimensional calculations.
7. The critical mass of nuclear fuel indicated by one-dimensional calculations for a 6-ft-diameter spherical cavity was approximately equal to that indicated by two-dimensional calculations for an equivalent cylinder having a length and diameter of 6 ft, whereas simplified theory for configurations with semi-infinite reflectors indicates that the critical mass for the cylinder should be 1.5 times that for the sphere.

INTRODUCTION

Reference engine design studies for a specific vortex-stabilized gaseous nuclear rocket were carried out at the Research Laboratories during fiscal year 1966. These studies took into consideration such factors as reflector-moderator heat balance, required coolant voids, selection of materials for the cavity inner liner and plumbing, manifolding and heat exchanger structures, selection of coolant fluids, exhaust nozzle geometry, pressure vessel configuration, and over-all engine weight. All of these factors interact with the nucleonics of the engine and affect the critical mass required. The engine design work is reported in Ref. 1, while the nuclear work on the reference engine design is reported herein.

Calculations of critical masses required in cavity reactors were reported first in Refs. 2 and 3, and further work has been reported in Refs. 4 through 13. Experimental measurements of critical mass requirements for selected cavity reactor configurations are reported in Refs. 14 and 15. In most instances, both the analytical work and the experimental measurements were made for idealized spherical cavities or for cylindrical configurations with length-to-diameter ratios of 1.0. Moderator materials employed for these measurements and calculations were also ideal (no voids for coolant or propellant passage and no structural materials) and were graphite, beryllium oxide, heavy water, or combinations of these three containing little or no neutron poisons. However, some calculations and measurements have been performed which include factors which should be considered in cavity reactors for nuclear rocket applications. In particular, calculations have been made which include the effects on critical mass resulting from the addition of heat- and pressure-resistant lining materials on the inner cavity wall (Refs. 6, 10, and 13) and by the presence of an exhaust nozzle penetrating the reflector-moderator (Refs. 7 and 8). In addition, experimental measurements have been made of the effects of an exhaust nozzle penetrating the reflector-moderator of a heavy-water-reflected cavity (Ref. 14). Additional calculations have been performed to estimate the effects of hot hydrogen on the neutron spectra and critical masses for cavity reactors (Ref. 11). The present study is the first attempt to calculate critical mass requirements for a specific engine design which includes coolant voids, plumbing structure, cavity lining material, exhaust nozzle holes penetrating the reflector-moderator and pressure vessel, hot hydrogen, a specific fuel density profile, and a fuel injection duct surrounded by a sleeve made of a strong neutron poison to prevent excessive heating of the fuel and local moderator volume during fuel injection.

STEPS IN NUCLEAR ANALYSIS

The nuclear calculations proceeded in four basic steps. First, engine configurations were selected in both one- and two-dimensional geometry with materials, material temperatures, and region dimensions chosen on the basis of the reference engine design study. The selected configurations consisted of a spherical geometry with a cavity of the same diameter as the cylindrical cavity in the reference engine design, a cylindrical geometry with length equal to diameter but having neither an exhaust nozzle port nor a fuel injection duct, and finally a cylindrical geometry which approximated the geometry of the reference engine design and which included both exhaust nozzle and fuel injection duct.

Secondly, three sets of neutron cross sections were established. Since the reference engine design contained reflector-moderator materials at different temperatures, hot hydrogen at a very high temperature between the cavity wall and the fuel region, and a fuel region with a density profile which varied linearly with radius, it was necessary to start calculations with cross section libraries containing 24 neutron energy groups. Of these 24 neutron energy groups, 14 were in the thermal neutron energy range from 0 to 29 electron volts with both up- and down-scattering probabilities within this range. The multi-thermal-group cross sections in the 24-group set were used only in the spherical one-dimensional calculations. A second set of flux and volume-weighted cross sections consisting of 4 neutron energy groups were generated from the multi-thermal-group, one-dimensional calculations for use in two-dimensional calculations. The third set of cross sections contained 14 neutron energy groups with down-scattering probabilities only. The thermal group cross sections of the 14-group set were those used in group 4 of the 4-group set.

Thirdly, a one-dimensional diffusion theory multi-group code with neutron slowing down only was used to do parameter surveys to establish trends in critical mass variations with variations in moderator voids, liner materials, structure materials, liner thicknesses, and moderator thicknesses. The 14-group cross sections were used for the parameter survey.

The final step of the nuclear study consisted of the critical mass calculations for two-dimensional configurations which included a two-dimensional cylinder without nozzle or fuel injection duct and two-dimensional configurations including exhaust nozzles and fuel injection duct with various amounts of structure materials in the nozzle area.

ENGINE SPECIFICATIONS AND NUCLEAR CONFIGURATIONS

The reference engine design used as a basis for nuclear criticality calculations is described in Ref. 1. A preliminary layout of the engine is shown in Fig. 1. The configurations used to approximate the compositions, dimensions, and geometry of the conceptual engine design for nuclear calculations agree in essential details with the final design of Ref. 1 with the exception that substantially greater masses of natural tungsten and steel in the heat exchanger and pressure vessel regions, respectively, were used in the nuclear calculations. It was assumed that the effect on critical mass due to reflection of either fast or thermal neutrons by the over-estimation of material mass in the two outermost regions was negligible for the following reasons. First, the fast neutron flux reaching these regions after traversal of the reflector-moderator was negligible. Secondly, the albedo for reflection of thermal neutrons by natural tungsten is less than 0.5%. Finally, the natural tungsten region was from 1 to 2 thermal neutron absorption mean-free-paths thick, so that reflection of thermal neutrons by the outer steel pressure vessel with an albedo of about 40% is diminished by thermal neutron absorption in the natural tungsten.

For a well reflected cavity, the required critical fuel densities are approximately equal for a sphere and for a cylinder of the same diameter, the cylinder having equal length and diameter. Therefore, an equivalent spherical configuration was chosen with a diameter equal to 6 ft and with the various thicknesses of liner, moderator, plenum, heat exchanger, and pressure shell equal to those for the reference engine design. The equivalent spherical configuration is shown in Fig. 2. The dimensions and volumes of the various regions in the spherical configuration are shown in Table I. The fuel-containing region is divided into three regions of equal volume. There are two regions of hydrogen: first a region adjacent to the fuel which is at very high temperature and pressure, namely 100,000 R and 1000 atmospheres; the second hydrogen region is a cool region adjacent to the cavity liner 2.0 in. thick and at a temperature of 5400 R. The next region is the cavity liner which consists of tiny W-184 tubes cooled internally by helium plus a beryllium containment vessel to prevent intercommunication of the helium coolant which passes through the reflector-moderator and the hydrogen propellant within the cavity. The next four regions are reflector-moderator regions consisting of beryllium oxide, graphite, a beryllium metal tank wall, and heavy water in that order. The thicknesses of these various regions were chosen on the basis of maximum temperature tolerances and heat balance considerations. Heating of the reflector-moderator regions was considered to be due exclusively to neutron and gamma volumetric heat deposition. The final two regions are a region containing the outer heavy water beryllium tank, natural tungsten manifolding, and plumbing for the various coolant cycles, heat exchangers, and propellant feed lines, and finally a steel pressure vessel. In addition to the dimensions and volumes of the various regions, Table I also indicates the number of radial mesh points employed in nuclear calculations and the material temperatures assumed for each region.

A two-dimensional cylindrical configuration which was used to approximate the reference engine design with no nozzle and no fuel injection duct is shown in Fig. 3. The dimensions and materials used for the two-dimensional cylinder shown in Fig. 3 are the same as those for the equivalent sphere in all regions except the fuel region and the hot hydrogen region adjacent to the fuel. The compositions of the various materials in both the one- and two-dimensional configurations are identical. Table II contains the compositions in the various regions for both the one- and two-dimensional cases while Table III contains the dimensions of the two-dimensional configuration. Note that in Table II the volume fractions in most regions do not add up to 1.0, thus allowing for voids filled with helium coolant. The presence of helium was neglected in the nuclear calculations because of its small scattering cross section and negligible thermal neutron absorption cross section. Table III also indicates the number of axial and radial mesh points employed for each region and the material temperatures assumed for each region. The numbers of mesh points in the axial and radial directions are additive so that a total of $25 \times 37 = 925$ mesh points were used in the nuclear calculations for the cylindrical configuration with no nozzle or fuel injection duct.

The reason for the different fuel region thicknesses in the two-dimensional configuration as compared to the one-dimensional is that in the cylindrical configuration the fuel density profile was considered to vary linearly with radius but was considered to be constant in the axial direction. Since the two-dimensional configuration is the actual engine design for which criticality calculations were to be performed, the fuel densities and fuel region volumes were calculated first for the cylinder. The spherical volumes were then made to conform to those for the cylinder. In order to do this, the radii of the fuel regions in the sphere had to be different from those in the cylinder; since the outer fuel radius was different for the sphere, then the thickness of the hot hydrogen layer for the spherical geometry also had to be commensurately less than for the case of the cylindrical geometry.

In order to represent the entire engine design, it was necessary to provide for exhaust nozzle penetration through one end of the cylinder and for a fuel injection duct through the other end. Figure 4 shows the assumed approximation of the exhaust nozzle geometry. In order to minimize the size of the penetration through the pressure shell, it was assumed that the nozzle had 15-deg-convergent and 30-deg-divergent cones and that these approach and exhaust cones were both contained within the thickness of the pressure vessel. The exhaust nozzle was then assumed to be an annular slot through the pressure vessel with the volume of void equal to the total void volume in the six exhaust nozzles of the reference engine design. Since the nozzle was embedded in the pressure vessel, a rather long nozzle approach was inserted in the form of a annular slot, equal in thickness to the hydrogen region between the fuel and the cavity wall. The material surrounding the exhaust nozzle was assumed to be of sufficient volume to allow transpiration cooling in the nozzle throat and in the convergent and divergent parts of the nozzle. The large annular slot leading toward the nozzle approach was assumed

CONFIDENTIAL

to be lined in one case with the same materials that lined the inner cavity wall (a combination of W-184 and beryllium), and in another with pure W-184.

The fuel injection duct geometry was chosen to be that used in Ref. 16, namely a hafnium sleeve one-half-inch thick surrounding an injection hole 0.08 in. in diameter. The geometry of the fuel injection duct is shown in Fig. 5.

The dimensions of the exhaust nozzle and fuel injection duct and the compositions of the materials within these two regions are given in Tables IV and V, respectively.

As was mentioned previously, the fuel concentration in the conceptual engine design was assumed to vary linearly with radius from the centerline peak concentration to zero concentration at the edge of the fuel cloud. The cylindrical fuel region was divided into three equal volumes. Figure 6 depicts the fuel concentration profile and the average fuel densities in each of the three fuel volumes which were used to simulate the real density profile. The differences in region radii between the cylindrical and spherical geometry were necessary to assure that both geometries were divided into three regions of equal volume.

The fuel and hot hydrogen were assumed to be at a temperature of 100,000 R and a pressure of 1000 atmospheres. Under these conditions, the fuel is approximately triply ionized, and the hydrogen is totally ionized. Since there is a fuel concentration profile, the concentration of hydrogen also varies with radius. In order to estimate this variation of hydrogen density with radius with relation to the fuel density profile, it was assumed that the total particle density within the fuel region was constant at 1.32×10^{20} particles per cubic centimeter. Figure 7 is a plot of hydrogen ion density versus fuel ion density for the assumed cavity temperature and pressure conditions. Ratios of hydrogen concentrations to fuel ion concentrations were used from this figure for the three different fuel regions in each calculation.

For the two regions containing hydrogen alone, the concentrations, partial pressures, and total hydrogen atom densities for H_2 , H, and H^+ were taken from Ref. 17 and indicated in Table VI for the various temperatures and pressures used in this study.

Finally, the densities and weights of all materials employed in the various reactor criticality calculations are summarized in Table VII. Table VII contains the atom densities and the mass densities of the various materials plus a summary of the total mass of the various materials used for the spherical one-dimensional geometry, the two-dimensional cylindrical geometry with no nozzle and no fuel injection duct, the cylindrical two-dimensional geometry with a nozzle and a fuel injection duct using the W-184 nozzle approach liner, and the two-dimensional geometry with nozzle and with fuel injection duct using the cavity liner material for the approach to the nozzle. As was noted previously, the very large amount of iron in the pressure vessel and the large amount of natural tungsten assumed to

CONFIDENTIAL

REFLECTOR-MODERATOR REGION
[REDACTED]

be in the heat exchanger and plumbing region between the reflector-moderator and the pressure shell would not reflect a significant number of neutrons and therefore did not affect the criticality calculations substantially.

NEUTRON CROSS SECTIONS

Selection of the neutron energy group structure and cross section sets was governed primarily by the different temperatures which were employed in the solid parts of the engine configurations and the presence of hot hydrogen in the fuel region. In order to calculate neutron absorptions and spectra accurately for adjacent regions in the reflector-moderator at quite different temperatures, it was necessary to employ several thermal neutron energy groups in the range from 0 to 1.125 electron volts. In addition, in order to calculate the effects of neutron up-scattering by the presence of hydrogen at 100,000 R in the cavity, it was also necessary to add several thermal neutron energy groups in the range between 1.125 and 29 electron volts. Thus, a basic set of 24 neutron energy groups was chosen with 14 of the groups covering the range from 0 to 29 electron volts and the remaining groups covering the range from 29 to 10^7 electron volts. Table VIII contains the energy boundaries of the 24-group structure. The fast neutron cross sections were calculated using the GAM-I code (Ref. 18) with slowing down spectra calculated for the various local moderator materials. The slowing down spectrum for the cavity region was assumed to be that of the beryllium oxide, the material in largest quantity adjacent to the cavity. Thermal neutron absorption cross sections were calculated using the TEMPEST code (Ref. 19) with the spectra chosen again for the temperatures and materials of the local moderator regions. Thermal neutron cross sections for the cavity region were calculated using the thermal neutron spectrum of beryllium oxide. Up- and down-scattering probabilities within the thermal neutron groups were calculated using the SOPHIST-I code (Ref. 20) which uses a Maxwellian distribution of moderator scattering atoms and an input neutron spectrum also assumed to be Maxwellian at the neutron temperature of the moderator with a $1/E$ tail at the nearest energy group boundary to $5 kT_n$. T_n is the neutron temperature and is assumed to be equal to the material temperature for all regions except those within the cavity. The SOPHIST-I code includes in the up- and down-scattering probabilities the enhancement of reaction rates due to relative velocity. The transport cross sections for the various materials were calculated by including this enhancement of reaction rate by the relative velocity effects in all regions. Thus the transport cross section is given by

$$\sigma_{tr1} = \sigma_{a1} + \sum_{j=1}^{15} \mu_{1j} \sigma_{s1} (1 - \overline{\cos \theta}) \quad (1)$$

where the sum of the μ_{1j} is the sum of the up- and down-scattering probabilities from energy group 1 to all other energy groups j , and $\overline{\cos \theta}$ is the mean value of the cosine of the scattering angle.

Treatment of Hot Hydrogen Scattering

The calculation of cross sections for the molecular hydrogen boundary layer between the hot hydrogen and the cavity wall and the hot ionized hydrogen at 100,000 R required special treatment. First, the hot hydrogen at 100,000 R can be assumed to be completely ionized and dissociated. Therefore, its scattering cross section is constant at 20 barns over all of the thermal neutron energy ranges. The SOPHIST-I code included the relative velocity effects in calculating enhanced reaction rates for up- and down-scattering probabilities. However, in calculating the transport cross section, not only must the relative velocity enhancement of scattering rate be included, but also some estimate must be made of the mean cosine of the scattering angle. In the special case where the hydrogen in the cavity is moving faster than the neutrons flowing into the cavity, the average angle of scattering in the laboratory system is nearly equal to that in the center of mass system. Therefore, in the limit for a very slow-moving neutron colliding with hydrogen moving at a very high speed, the scattering may be considered isotropic, i.e., the mean cosine of the scattering angle may be considered to be zero. Treatment of mean scattering angle has been reported in Ref. 21 where $(1 - \overline{\cos \theta})$ was calculated for atomic hydrogen gas as a function of the ratio of the speed of a colliding particle to the most probable speed of a similar particle in a Maxwellian distribution. A plot of $(1 - \overline{\cos \theta})$ vs the ratio of neutron velocity to the most probable velocity of atomic hydrogen is shown in Fig. 8. These values were used to calculate the transport cross section by the equation:

$$\sigma_{tr_i} = \sigma_{s_i} + \sum_{j=1}^{15} \mu_{ij} \sigma_{s_j} (1 - \overline{\cos \theta})_i \quad (2)$$

Equation (2) is the same as Eq. (1) with the addition of group dependence in the $(1 - \overline{\cos \theta})$ term. Table IX contains atomic hydrogen cross sections for the various hydrogen temperatures used.

It should be noted that transport cross sections for atomic hydrogen were calculated for temperatures of 100,000 R and 20,000 R. At 20,000 R and 1000 atmospheres, the hydrogen environment contains a mixture of atomic and molecular hydrogen. Further complications in the transport cross section for hydrogen occur due to two factors when molecular hydrogen is present. First, the reduced mass of the neutron-hydrogen scattering system increases for neutron energies well below the binding energy of molecular hydrogen (~ 4.5 ev) because the hydrogen scattering center has a mass twice that of atomic hydrogen. As a result, the hydrogen scattering cross section per atom increases for molecular hydrogen. Secondly, because the effective mass of the molecular hydrogen scattering center approaches a value twice that of the neutron, the mean cosine of the scattering angle is different from that for atomic hydrogen. No calculated or measured data was found for values of $(1 - \overline{\cos \theta})$ for scattering interactions between thermal neutrons and molecular hydrogen. Therefore, for neutron energies well below the binding energy of hydrogen, ~ 4.5 ev, it was assumed that the value of $\overline{\cos \theta}$ was

half that for atomic hydrogen. For energies between the range of 1 and 4 ev, the limit of $(1 - \overline{\cos \theta})$ was varied linearly with energy from 0.667 to 0.333. Figure 8 contains the limiting values of $(1 - \overline{\cos \theta})$ for both molecular and atomic hydrogen. Table X contains the hydrogen transport cross sections for molecular hydrogen at the two temperatures employed, 20,000 R and 5400 R. The scattering cross sections per atom for molecular hydrogen shown in Table X are measured values corrected for thermal motion from Ref. 22 for the average energy of each energy group. Figure 9 contains plots of scattering cross section per atom versus energy for molecular hydrogen reproduced from Ref. 22. There was assumed to be no atomic hydrogen in the environment of hydrogen at 5400 R.

It is significant to note that, for atomic hydrogen at 20,000 R to 100,000 R, transport cross sections in the very low energy groups below 0.1 ev (groups 22 to 24) are as much as an order of magnitude greater than the transport cross sections at the energies corresponding to the average neutron energy at that temperature (groups 12 to 15). This means that not only is there a great deal of up-scattering of the neutrons in the low energy groups to higher energies, but that also the low-energy neutrons experience a great deal of difficulty in diffusing across the hot hydrogen regions.

Comparison of 24-Group and 4-Group Cross Sections

In order to calculate two-dimensional configurations economically, the 24-group cross sections used in the one-dimensional spherical calculations were used to generate volume- and flux-weighted 4-group cross sections. The neutron energy boundaries of the 4-group set are shown in Table VIII. In order to evaluate the accuracy of the 4-group set, companion problems were run for the spherical one-dimensional case in which a 24-group calculation was compared with a 4-group calculation for identical fuel loadings and identical geometry. Table XI contains a comparison of the neutron balances from these two calculations. It can be seen that k_{eff} , peak to average power, fuel absorptions per fission, and neutron source calculations correspond very closely for the two calculations. Neutron leakages and absorptions within the cavity also correspond closely for the two calculations. The major differences occur in the fast fluxes and total fluxes and in comparison of absorptions in the reflector-moderator. The cause of these differences is attributed primarily to the inability of the 4-group cross sections to calculate accurately the communication of neutrons between low energy groups in the reflector-moderator materials adjacent to one another and at different temperatures. However, since the two sets of cross sections calculate cavity conditions accurately, the discrepancies in absorption and total fluxes in the reflector-moderators do not affect the calculation of k_{eff} or critical fuel loading significantly, so it was assumed that the 4-group cross section set could be used to calculate critical masses for two-dimensional geometries.

RESULTS OF ONE-DIMENSIONAL DIFFUSION THEORY CALCULATIONS

24-Group Calculations

One-dimensional criticality calculations were performed using two different neutron diffusion theory codes. The first set of calculations was made for the spherical configuration whose dimensions and compositions are given in Tables I and II, using the ULCER one-dimensional diffusion theory code (Ref. 23) and the 24-group cross sections. The principal objective of these calculations was to develop flux- and volume-weighted 4-group cross sections for two-dimensional calculations. In addition to generation of 4-group cross sections, critical mass variations were calculated for changes in fuel density profiles within the spherical configuration, changes in fuel-containing volume, changes in the thickness of cool hydrogen layer adjacent to the cavity liner, and for different nuclear fuels. Figure 10 shows the results of U-233 critical mass calculations for both the uniform-fuel-density profile (yielding a 35.25-lb critical mass) and for the stepped-density profile (39.25-lb critical mass), in which the fuel-bearing region was divided into three equal volumes. The fuel-density profile for the stepped fuel loading is that shown in Fig. 6 for the spherical configuration. This increase in critical mass for the stepped fuel density profile is attributed to self-shielding of the high-density central fuel region, and to greater alteration of the spectrum of neutrons flowing into the central fuel region due to a larger effective thickness of hot hydrogen.

The neutron flux spectra from the 24-group calculations are shown in Fig. 11. The six flux plots are shown for the three principal reflector-moderator regions and for three regions within the cavity. The different flux spectra show the changes in neutron distribution with the temperature of the various reflector-moderator regions and the marked effect of hydrogen up-scattering on the neutron spectrum in the cavity. It can be seen, for example, that, in the hot-hydrogen region where the hydrogen temperature is 100,000 R, the neutron spectrum peak is only 40% of the peak value of the flux in the beryllium oxide region. In addition to the flux spectra, the growth of integrated flux with energy is shown for the beryllium oxide and fuel regions in Fig. 11. It can be seen from these plots that the presence of the hot hydrogen causes the ratio of group-3 to group-4 integrated fluxes to be 0.62 in the fuel region as compared to 0.20 in the beryllium oxide region.

It is fortunate in the case of U-233 that there are several fission resonances between 1 and 5 electron volts so that up-scattering of neutrons within the cavity does not affect critical mass requirements dramatically. This is not the case when U-235 or Pu-239 fuels are used. In order to compare U-233 critical mass requirements with those of U-235 and Pu-239, calculations using 24-group cross sections were made for the one-dimensional equivalent spherical geometry using U-235 and Pu-239. The results of these calculations are shown in Table XII and indicate that the critical mass for U-235 is 120.0 lb and for Pu-239 is 149.5 lb as compared to critical mass requirement of 37.25 lb for U-233 in the identical spherical geometry.

Two other sets of 24-group one-dimensional calculations were performed using U-233 fuel with the stepped density profile. The first of these sets demonstrates the effect of fuel volume variation on critical mass requirements. The results of these calculations are shown in Fig. 12. For these cases, the fuel-containing volume was varied from 0.80 to 1.20 times that of the basic case. The variation of critical mass over this range of fuel volumes was from about 38.6 lb of U-233 for the smallest fuel volume to about 36.7 lb of U-233 when the fuel-bearing volume was 1.20 times that of the basic case. Two factors contribute to these variations in critical mass with fuel volume variation: the first is an increase in self-shielding as the fuel volume is collapsed, and the second is an increase in the thickness of the hot hydrogen layer between the cavity wall and the fuel which causes greater changes in the spectrum of neutrons entering the fuel region.

The variation of critical mass requirements with the thickness of the cool hydrogen layer adjacent to the cavity wall is shown in Fig. 13. For these calculations, the thickness of the molecular hydrogen layer at 5400 R was varied from 1 to 3 in. The critical mass requirement over this range varied from 40.0 lb for the 1-in.-thick layer to about 34.9 lb for the 3-in.-thick layer. This decrease in critical mass with increased molecular hydrogen boundary layer thickness is attributed to an increase in the slowing down power of the reflector-moderator as more cold hydrogen is placed adjacent to the cavity wall.

These last two results have interesting effects on the transient behavior of nuclear rocket cavity reactors. For example, a decrease in fuel region volume would lead to a cooling of the hydrogen region since the reactivity of the system would go subcritical. The cooling of the hydrogen region would tend to cause the molecular hydrogen layer at the cavity boundary to grow, inserting a positive reactivity effect. Further analysis is necessary to determine whether the positive effect of the growth of the molecular hydrogen layer could override the negative reactivity effect of a collapsing fuel volume.

14-Group Calculations

Additional one-dimensional calculations for the basic spherical geometry were made using the FAIM one-dimensional diffusion theory code which provides only for neutron slowing down (Ref. 24). Fast neutron energy groups from the standard 18-group neutron cross section library for the FAIM code were coupled to the thermal group cross sections between 0 and 1.125 ev which were generated by the ULCER calculations, thus yielding a 14-group cross section library. The one-dimensional calculations were performed to guide the choices of materials and moderator coolant schemes employed in the reference design study. Calculations were performed to examine the effects of void fraction, variation of inner liner thickness, moderator zone thicknesses, and W-184 enrichment on the U-233 critical mass. The void fraction in the moderator region consists of the coolant passages through which the helium coolant must pass to remove the volumetric heat load in each region,

passages through which hydrogen propellant is transmitted to the cavity, and tolerance allowances in piecing together segments of the moderator. Critical mass calculations were performed in which the void fractions in each of these regions were varied separately from zero to twice that required for the reference engine design, and for a final case in which the void fractions in all three regions were varied simultaneously from zero to twice those required in the reference engine design. These results are shown in Figs. 14 through 17. Figures 14 through 16 show the results for variations in void fraction in the beryllium oxide, graphite, and heavy water regions, respectively. Over the range from zero void fraction to twice that required by the reference design, the critical mass does not vary by more than 5%, the effect of variation in void fraction in the beryllium oxide region being the greatest. On the other hand, when the void fraction is varied simultaneously in all three reflector-moderator regions, the results shown on Fig. 17 indicate that critical mass can vary by 30% over the range from zero void fraction to twice that required by the spherical analogue of the reference design. For purposes of comparison, the critical mass of the 14-group FAIM calculation was 36.8 lb while that for the 24-group ULCER calculation was 35.25 lb for the basic spherical configuration with a uniform fuel density profile. The use of a uniform fuel density profile was necessitated in the FAIM calculations by a limitation to ten material regions instead of the twelve regions allowed in ULCER. The reason for agreement to within about 4.4% between the 24- and 14-group calculations is that U-233 is relatively insensitive to transfer of neutrons by up-scattering interactions across the 1.125 ev boundary of the thermal neutron energy group of the 14-group cross sections. For any fuel other than U-233, agreement between the two codes would not be expected to be as good.

In order to evaluate the effect of the thickness of a W-184 tube liner along the cavity wall, the density of W-184 in that liner was varied from zero to 10 times the reference design density. The results of these calculations are shown in Fig. 18. The principal result is that the basic liner for the equivalent spherical configuration causes an increase in critical mass relative to that with no liner by approximately 60%. The rapid increase in critical mass as the liner density increases from 5 to 10 times that of the basic case indicates that a liner of thickness much greater than that used in the conceptual engine design cannot be tolerated. In fact, the increase in critical mass due to the W-184 liner employed for the first reference design has motivated plans for a second design (see Ref. 1) which would employ a liner configuration in which beryllium tubes were covered with niobium-carbide-coated pyrolytic graphite; such a configuration would provide far less neutron poisoning than tubes made from W-184.

The rather high critical masses with the basic reflector-moderator configuration lead to an investigation of the effect of the thickness of the heavy-water region on U-233 critical mass. The results of these calculations are shown in Fig. 19. It can be seen that doubling the heavy water region thickness can reduce critical mass requirements by about 25%. In addition to reducing the critical mass requirements, the use of a thicker reflector-moderator would also reduce the sensitivity of the


system to liner thickness, liner neutron poison, and the presence of structural poisons in the reflector-moderator regions. However, as can be seen from Fig. 19, there is a considerable weight penalty involved in increasing the thickness of the heavy water region. In addition to the added weight of heavy water created by doubling the thickness of this region, the weight of the pressure shell would also increase substantially due to the increased over-all size of the rocket engine.

The reference engine design employed tungsten as a high-temperature material. The tungsten employed in moderator regions was pure ^{184}W isotope, since natural tungsten has a thermal neutron absorption cross section about an order of magnitude larger than that for the ^{184}W isotope. However, W-184 is extremely expensive to obtain in high purities. Therefore calculations were made to investigate the effect of the W-184 enrichment on critical mass in the spherical configuration using the structural materials established for the reference engine design. The results of these calculations, shown in Fig. 20, indicate that W-184 enrichment must be equal to or higher than 97.5% to limit the increase in critical mass due to addition of natural tungsten to less than 15%.

The results of the 14-group one-dimensional calculations lead to estimates of critical mass considerably greater than employed in earlier studies (Ref. 25). Table XIII contains a summary of the critical mass buildup and attempts to indicate the causes for this increase in critical mass. This table shows critical mass requirements as various factors affecting the critical mass are added to the configuration. Starting with a critical mass of 16.4 lb for a spherical configuration containing fuel and hot hydrogen at 500 atm and 100,000 R and with idealized reflector-moderator regions with material densities considerably above those used in the reference engine design, it can be seen that by systematic introduction of factors affecting critical mass such as an increase in cavity pressure, decreases in reflector-moderator densities to accommodate voids for coolant and propellant, addition of a W-184 heat-resistant cavity liner, and the use of W-184 plumbing structure, critical mass is increased to 36.8 lb. It can be seen from these tabulated results that one of the major causes for critical mass buildup is the presence of the W-184 liner in the cavity. The next most important factor appears to be the introduction of voids in the reflector-moderator regions.

Further calculations to duplicate the results of the Corporate-sponsored calculations which were used for the critical mass estimates employed in Ref. 25 were not attempted because generation of cross sections for different moderator temperatures and hot hydrogen temperatures would have been necessary. Furthermore, the 14-group calculations used to obtain the results of Table XIII yielded critical mass about 4.4% higher than the companion 24-group calculation for the spherical analogue of the reference engine design.

The critical mass employed for the studies of Ref. 25 was estimated by multiplying the critical mass for the spherical configuration shown in the first row of Table XIII (12.3 lb) by a factor of $3/2$ to obtain the critical


mass requirements for a cylindrical configuration of equal length and diameter and with a cavity diameter equal to that of the sphere. It is shown in the next section that this method of estimating critical mass for a cylindrical configuration does not appear to be valid when there is appreciable neutron leakage from the reflector-moderator.

RESULTS OF TWO-DIMENSIONAL DIFFUSION THEORY CALCULATIONS

Two-dimensional diffusion theory calculations of U-233 critical mass requirements using the TWENTY GRAND code (Ref. 26) were made for a cylindrical geometry using three different assumptions concerning the nozzle and fuel-injection duct: no nozzle and no fuel-injection duct; with a fuel-injection duct and nozzles penetrating the reflector-moderator and pressure shell; and with nozzle and fuel injection ducts but with less W-184 structure in the nozzle-approach region. The results of the two-dimensional calculation for the case with no nozzle and no fuel injection duct are shown in Fig. 21. The critical mass requirements for this configuration amount to 35.7 lb of U-233. This mass is considerably less than that projected from the one-dimensional calculations, and the difference is attributed to less leakage from the two-dimensional configuration than was calculated for the one-dimensional equivalent sphere and a lower ratio of fast-to-thermal neutron flux in the cylindrical configuration. Figure 22 contains midplane radial neutron flux plots for all four energy groups for both the cylindrical configuration with no nozzle or fuel-injection duct and the equivalent spherical configuration. Both sets of fluxes are normalized such that the peak values are 1 neutron/cm²-sec. It can be seen that the ratio of group-1 flux to group-4 flux in the fuel region for the cylindrical configuration is approximately 1.0 while for the equivalent sphere it is about 1.5. Furthermore, the group-3 flux in the fuel region in the cylinder is nearly twice that in the sphere. Thus, the cylindrical configuration exhibits a considerably softer neutron flux in the cavity than does the spherical configuration with the same cavity diameter and identical reflector-moderator thickness and composition.

Table XIV contains comparisons of neutron absorptions per region for the two geometries. It can be seen from this table that the absorptions in (and hence neutron leakages into the natural tungsten and iron pressure vessel for) the spherical configuration are greater than those for the two-dimensional calculations. Also, the ratio of neutron absorptions in the outer two regions to absorptions in the reflector-moderator regions for the spherical configuration is 1.5 times the same ratio for the cylinder. It can be concluded from these results that the analogy which states that critical fuel density for spheres and cylinders with equal length and diameter should be identical is not good for cases in which the reflector-moderator is not a semi-infinite region. That is to say, the analogy between an equivalent sphere and a cylindrical cavity with a length to diameter ratio of 1 is good only in those cases where a large and highly efficient reflector-moderator is employed.

Figures 22 and 23 contain midplane radial neutron flux plots and centerline axial neutron flux plots for the cylindrical configurations with no nozzles. The shapes of these flux plots are typical of cavity reactors. Neutron group-4 (thermal) flux peaks in the reflector-moderator region and is depressed slightly as the radius approaches zero in the fuel region. The group-3 flux, which extends from 1.125 to

[REDACTED]

29 ev, builds up only slightly in the reflector-moderator region and is depressed similarly to the group-4 flux in the fuel region. The group-1 and group-2 fluxes exhibit slowing down spectra in the reflector-moderator region as might be expected and are relatively flat in the diffuse cavity region.

The results of two-dimensional diffusion theory calculations for the reference engine design with exhaust nozzles and fuel injection duct are shown in Fig. 24. Two different exhaust nozzle approach liners were used; one consisting of pure W-184 with an effective thickness of 0.17 thermal neutron absorption mean-free-paths, and the other consisting of internally cooled W-184 tubes such as those used for the cavity liner with an effective thickness of 5.8×10^{-3} thermal neutron mean-free-paths. The latter configuration with the W-184 tubes lining the exhaust nozzle approach is referred to as the reference engine design, and the configuration with the pure W-184 exhaust nozzle approach liner is considered a modified version of the reference engine design. The fuel injection duct geometries and the exhaust nozzle geometry are shown in Figs. 5 and 6, while the dimensions and compositions for all regions are given in Tables I, II, IV, and V. The fuel injection duct was assumed to be a black absorber in group-3 and group-4, while in group-1 and group-2 the regular hafnium fast-group cross sections were employed. In order to simulate neutron streaming leakage from the exhaust nozzle region, a black absorber was placed adjacent to the end of the reactor configuration containing the nozzle annulus. This use of a black absorber for all neutron energy groups at this position provided neutron flux gradients which were governed by the diffusion coefficients of the regions adjacent to the black absorber, namely, the diffusion coefficients of iron for the pressure vessel and the large diffusion coefficients for the hydrogen in the nozzle throat annular slot.

Two different exhaust nozzle approach liners were used for the reference design configuration. The first calculation was for the modified reference engine design with W-184 for the exhaust nozzle lining material, resulting in a critical mass of 60.9 lb. The next calculation was performed for the reference engine design in which the nozzle approach liner was constructed of the same W-184 tubes used for the cavity inner liner. This change reduced the critical mass to 50.1 lb. If comparison of these results is made to the two-dimensional calculation with no nozzles and no fuel injection duct, it must be concluded that the presence of the annular nozzle approach slot and the fuel injection duct causes an increase in critical mass from approximately 35.7 lb to 50.1 lb.

Figures 25 through 28 contain radial flux plots for the two-dimensional modified reference engine design. The first set of flux plots in Fig. 25 are taken through the fuel injection duct at an axial position which penetrates the graphite moderator region at its midpoint. It can be seen that the group-3 and group-4 fluxes are depressed by the presence of the fuel injection duct which is treated as a black absorber, while the group-1 and group-2 fluxes are relatively flat through both the graphite region and the hafnium injection duct. Figure 26 shows the midplane radial neutron flux distributions for the four energy groups employed. The comments regarding the flux distributions for the cylindrical configuration

with no nozzles apply to these flux distributions as well. Figure 27 contains radial neutron flux distributions through the axial midplane of the nozzle approach slot. It can be seen from these plots that the presence of a relatively thick region of W-184 as a lining material for the nozzle approach depresses the group-4 flux considerably. This is why the critical mass for the configuration using W-184 in the nozzle approach is about 20% larger than for the reference engine design in which the nozzle approach liner is made of the same tiny W-184 tubes employed in the cavity liner. It can also be seen from these flux plots that the group-1 flux begins to peak in the nozzle approach slot, indicating a streaming of fast neutrons through the nozzle. The group-2 flux is only slightly affected by the presence of the nozzle approach liner and the 20,000 R hydrogen in the nozzle. The group-3 flux peaks in this region principally because of the presence of hydrogen at 20,000 R which tends to up-scatter the group-4 neutrons into group-3. The final radial flux plot for the modified reference engine design is shown in Fig. 28 and is plotted for the axial midplane of the nozzle throat. This plot shows the streaming of fast neutrons out through the nozzle very dramatically. It also shows a tendency for a peaking of the group-2, 3, and 4 fluxes. The odd shape of the group-2 flux can be attributed to resonance absorption of neutrons by the W-184.

Calculations were also performed to evaluate the effect of nozzle throat size on critical mass. These results are contained in Table XV. It can be seen that the width of the annular nozzle throat has little or no effect on critical mass. In fact, the values of k_{eff} for the cases in which the exhaust nozzle width was doubled and tripled were so close to k_{eff} for the modified reference design engine that the critical masses in Table XV were estimated by applying the ratio of $(\Delta k/k) \div (\Delta M_c/M_c)$. This result is not surprising, since the relative size of the area of the nozzle throat is extremely small, and since the tungsten surrounding the throat is such a poor reflector of neutrons.

Table XV contains a summary of the results of all the two-dimensional calculations. The results calculated are tabulated and show the increase in critical mass from the cylindrical geometry with no nozzle and no fuel injection duct to the critical mass for the configuration which includes the exhaust nozzle and fuel injection duct and the W-184 liner for the exhaust nozzle approach. Examination of these results indicate that a reduction of critical mass could be achieved by employing little or no W-184 and by reducing the volume of moderator material lost to the nozzle approach slot region. The highest value of critical mass, 60.9 lb, calculated for the modified reference engine design can be considered a pessimistic result. A critical mass of 46.3 lb was estimated for a configuration with no fuel injection duct but with the reference engine design exhaust nozzles with their approach slot lined with the cavity liner W-184 tubes. This mass was estimated using the criteria of the ratio of fuel injection duct surface area to cavity surface area from Table III of Ref. 16.

Table XVI contains a summary of the effect on U-233 critical mass resulting from changes in weights of moderator, propellant, and structural materials and by changes in dimensions of fuel, hydrogen, and moderator regions for both one- and

CONFIDENTIAL

[REDACTED]

two-dimensional calculations. The factors for the one-dimensional calculations are helpful in indicating the regions to which attention should be concentrated to reduce critical mass. For example, addition of beryllium oxide to the inner reflector-moderator region is of more worth than increasing the thickness of the outer heavy-water region. With regard to the variation of fuel volume and cool hydrogen layer, the growth in the cool hydrogen layer thickness need only be about 1/5 the reduction in fuel region radius to overcome the negative reactivity effect of fuel region collapse. Comparison of one- and two-dimensional mass change factors indicates that removal of moderator from a localized region such as the nozzle approach volume is worth approximately twice as much as uniform removal or addition of moderator in the spherical case. Results indicate that use of a nozzle approach volume one-half of that used in this study would reduce critical mass by 7.9 lb assuming linear behavior of $(\Delta M_c / M_c) + (\Delta M_{mod})$ for the cylindrical configuration.

Further work on conceptual engine design should include removal of all possible poisons from the reflector-moderator region, the use of high-density pyrolytic graphite in the high-temperature reflector-moderator region, and reduction of the volume of nozzle approach.

REFERENCES

1. McLafferty, G. H., H. E. Bauer, and D. E. Sheldon: Preliminary Conceptual Design Study of a Specific Vortex-Stabilized Gaseous Nuclear Rocket Engine. NASA CR-698, 1967. (Confidential, title unclassified)
2. Bell, G. I.: Calculations of the Critical Mass of UF_6 as a Gaseous Core with Reflectors of D_2O , Be, and C. Los Alamos Report LA-1874, February 1955.
3. Safonov, G.: The Criticality and Some Potentialities of Cavity Reactors. Rand Corporation Research Memorandum RM-1835, July 1955.
4. Safonov, G.: Engineering Test Reactors with Large Central Irradiation Cavities. Nuclear Science and Engineering, Vol. 2, No. 4, July 1957, p. 527.
5. Ragsdale, R. G. and R. E. Hyland: Some Nuclear Calculations of U-235 D_2O Gaseous Core Cavity Reactors. NASA TN D-475, October 1961.
6. Mills, C. B.: Reflector Moderated Reactors. Nuclear Science and Engineering, Vol. 13, No. 4, August 1962, p. 301.
7. Hyland, R. E., R. G. Ragsdale, and F. J. Gunn: Two-Dimensional Criticality Calculations of Gaseous-Core Cylindrical-Cavity Reactors. NASA TN D-1575, March 1963.
8. Holl, R. J. and T. F. Plunkett: Cavity Nuclear Reactors. Douglas Paper No. 1738, July 1963.
9. Hubbard, H. W., A. L. Latter, and E. A. Martinelli: Second Report on Propulsion by a Gaseous Fission Reactor. Rand Memorandum RM-3851-AEC, October 1963.
10. Butler, W. R., H. C. Chang, and J. A. Vreeband: A Transport Theory Analysis of a Gaseous Core Concept. Aerojet-General REON Report RN-TM-0190, May 1965.
11. Latham, T. S. and L. O. Herwig: The Effects of Hot Hydrogen Propellant on the Critical Mass of Gaseous Nuclear Rocket Cavity Reactors. AIAA Paper No. 65-564, AIAA Propulsion Joint Specialist Conference, June 1965.
12. Tumm, G. W.: U-235 Resonance Cross Sections and Gaseous Core Reactor Calculations. Plasma Research Laboratory Report No. 22, Columbia University, New York, August 1965.

[REDACTED]

REFERENCES (contd.)

13. Eriksen, J. A., R. M. Kaufman, W. F. Osborn, E. B. Roth, J. R. Simmons, and A. H. Foderaro: Gaseous-Fueled Cavity Reactors - Criticality Calculations and Analysis. General Motors Corporation, NASA CR-487, July 1966.
14. Byers, C. C.: Private Communication. Los Alamos Scientific Laboratory. Dec. 1961.
15. Jarvis, G. A. and C. C. Byers: Critical Mass Measurements for Various Fuel Configurations in the LASL D₂O Reflected Cavity Reactor. AIAA Paper No. 65-555, AIAA Propulsion Joint Specialist Conference, June 1965.
16. Latham, T. S.: Heat Generation in Nuclear Fuel During Injection Into a Gaseous Nuclear Rocket Engine. AIAA Paper No. 66-620, AIAA Second Propulsion Joint Specialist Conference, June 1966.
17. Krascella, N. L.: Tables of Composition, Opacity and Thermodynamic Properties of Hydrogen at High Temperatures. United Aircraft Research Laboratories Report B-910168-1, Contract No. NAS3-3382, September 1963.
18. Joanou, G. D. and J. S. Dudek: GAM-1, A Consistent P-1 Multigroup Code for the Calculation of Fast Neutron Spectra and Multigroup Constants. General Atomics Report GA-1850, June 1961.
19. Shudde, R. H. and J. Dyer: TEMPEST, A Neutron Thermalization Code. North American Aviation, September 1960.
20. Canfield, E. H., R. N. Stuart, R. P. Freis, and W. H. Collins: SOPHIST-I, An IBM 709/7090 Code Which Calculates Multigroup Transfer Coefficients for Gaseous Moderators. University of California Lawrence Radiation Laboratory Report UCRL-5956, Livermore, Calif., October 1961.
21. Desai, R. C. and M. Nelkin: Atomic Motions in a Rigid Sphere Gas as a Problem in Neutron Transport. Nuclear Science and Engineering, Vol. 24, No. 2, 1966, p. 142.
22. Melkonian, E.: Slow Neutron Velocity Spectrometer Studies of O₂, N₂, A, H₂, H₂O and Seven Hydrocarbons. Physical Review, Vol. 76, No. 12, December 15, 1949, p. 1750.
23. Vargofcak, D. S., W. T. Hayes, and D. W. Roeder: ULCER, A One-Dimensional Multigroup Diffusion Equation Code with Up-Scatter. Atomics International, NAA-SR-MEMO-9891, May 1964.
24. Baller, D. C.: The FAIM Code, A Multi-Group, One-Dimensional Diffusion Equation Code. Atomics International Report AMTD-118, January 1962.

REFERENCES (contd.)

25. McLafferty, G. H.: Analytical Study of the Performance Characteristics of Vortex-Stabilized Gaseous Nuclear Engines (Confidential - title unclassified). United Aircraft Research Laboratories Report D-910093-20, September 1965.
26. Tobias, M. L. and T. B. Fowler: The TWENTY GRAND Program for the Numerical Solution of Few-Group Neutron Diffusion Equations in Two-Dimensions. Oak Ridge National Laboratory Report ORNL-3200, February 1962.

LIST OF SYMBOLS

$\overline{\cos \theta}$	Mean cosine of neutron scattering angle, dimensionless
E	Neutron energy, ev
\overline{E}_i	Average energy of neutron energy group i, ev
ev	Energy, electron volts
k	Boltzmann's constant, erg/K
k_{eff}	Effective multiplication factor, dimensionless
M_c	Critical mass, lb or Kg
M_{mod}	Mass of all moderator materials, lb or Kg
M_x	Mass of material x, lb or Kg
m	Mass of hydrogen atom, gm
N_H	Atom density of all hydrogen species, atoms/cm ³
N_{H_2}	Atom density of molecular hydrogen, atoms/cm ³
N_{H+H+}	Atom density of atomic hydrogen and hydrogen ions, atoms/cm ³
N_U	Atom density of uranium, atoms/cm ³
P	Pressure, atm
P_H	Partial pressure of atomic hydrogen, atm
P_{H+}	Partial pressure of hydrogen ions, atm
P_{H_2}	Partial pressure of molecular hydrogen, atm
R	Radius, in. or cm
R_f	Fuel region radius, in. or cm
T	Temperature, R or K
T_H	Hydrogen temperature, R or K

LIST OF SYMBOLS (contd.)

T_n	Neutron temperature, R or K
\overline{V}_1	Average speed of neutrons in energy group 1, cm/sec
V_0	Most probable speed, cm/sec
$\mu_{i,j}$	Probability of neutron transfer from energy group i to energy group j by scattering interaction, dimensionless
ρ	Fuel density, gm/cm ³ or lb/ft ³
$\overline{\rho}$	Average fuel density, gm/cm ³ or lb/ft ³
ρ_0	Centerline fuel density, gm/cm ³ or lb/ft ³
σ_a	Neutron absorption cross section, barns
σ_s	Neutron scattering cross section, barns
σ_{tr}	Neutron transport cross section, barns
Φ	Integrated neutron flux, neutrons/cm ² -sec
ϕ	Differential neutron flux, neutrons/cm ² -sec-ev

TABLE I

DIMENSIONS OF REGIONS EMPLOYED IN BASIC ONE-DIMENSIONAL CALCULATIONS

Geometry Shown in Fig. 2
Composition of Regions Given in Table II

Region Description	No.	Radius of Region Outer Edge		Thickness of Region		Volume of Region		No. of Radial Mesh Points In Each Region	Temperature of Region	
		cm.	in.	cm.	in.	cm ³	ft ³		R	K
Inner Fuel Region	1	50.100	19.724	50.100	19.724	5.3×10^5	18.75	8	100,000	55,555
Center Fuel Region	2	63.100	24.843	13.000	5.119	5.26×10^5	18.57	4	100,000	55,555
Outer Fuel Region	3	72.200	28.425	9.100	3.582	5.24×10^5	18.51	3	100,000	55,555
Hot Hydrogen Layer	4	86.360	34.000	17.780	7.000	1.12×10^6	39.62	3	100,000	55,555
Cool Hydrogen Layer	5	92.44	36.000	5.080	2.000	5.05×10^5	17.82	3	5,400	3,000
Inner Liner	6	93.599	36.850	2.159	0.850	2.32×10^5	8.20	5	1,200	667
Beryllium Oxide	7	102.616	40.400	9.017	3.550	1.09×10^6	38.56	3	2,533	1,405
Graphite	8	124.841	49.150	22.225	8.750	3.63×10^6	128.0	5	4,067	2,260
Beryllium Vessel	9	126.365	49.750	1.524	0.600	3.02×10^5	10.67	3	1,200	667
Heavy Water	10	151.638	59.700	25.273	9.750	6.16×10^6	217.3	5	750	416
Tungsten Plumbing	11	165.100	65.000	13.462	5.300	4.25×10^6	149.9	3	1,000	555
Steel Pressure Shell	12	188.976	74.400	23.876	9.400	9.42×10^6	332.6	5	1,000	555

TABLE II

COMPOSITION OF REGIONS EMPLOYED IN BASIC ONE- AND TWO-DIMENSIONAL CALCULATIONS

Dimensions of Regions Given in Tables I and III

Region		Volume Fractions										
Description	No.	Nuclear Fuel	Hot Hydrogen	Cool Hydrogen	Beryllium	BeO	W-164	W-Mat	Graphite	Pyrolytic Graphite	Iron	Heavy Water
Inner Fuel Region	1	Varied	Varied	--	--	--	--	--	--	--	--	--
Center Fuel Region	2	Varied	Varied	--	--	--	--	--	--	--	--	--
Outer Fuel Region	3	Varied	Varied	--	--	--	--	--	--	--	--	--
Hot Hydrogen Layer	4	--	1.0	--	--	--	--	--	--	--	--	--
Cool Hydrogen Layer	5	--	--	1.0	--	--	--	--	--	--	--	--
Inner Liner	6	--	--	--	0.354	--	0.054	--	--	--	--	--
Beryllium Oxide	7	--	--	--	0.00184	0.9004	0.00076	--	--	0.006	--	--
Graphite	8	--	--	--	0.00136	--	0.00056	--	0.92268	0.0044	--	--
Beryllium Vessel	9	--	--	--	0.503	--	--	--	--	--	--	--
Heavy Water	10	--	--	--	0.00457	--	0.00215	--	--	--	--	0.94728
Tungsten Plumbing	11	--	--	--	0.048	--	--	0.167	--	--	--	--
Steel Pressure Shell	12	--	--	--	--	--	--	--	--	--	0.909	0.091

TABLE III

DIMENSIONS OF REGIONS EMPLOYED IN BASIC TWO-DIMENSIONAL CALCULATIONS

Geometry Shown in Fig. 3

Composition of Regions Given in Table I:

No.	Region	Radius of Outside Edge of Boundary of Region Parallel to Axis		Thickness of Region Parallel to Axis		Distance from Axis: Midplane to Outside Edge of Region Perpendicular to Axis		Thickness of Region Perpendicular to Axis		Total Volume of Region		No. of Radial Mesh Points in Each Region		No. of Axial Mesh Points in Each Region		Temperature, °K	
		in.	cm.	in.	cm.	in.	cm.	in.	cm.	in. ³	cm. ³	in.	cm.	in.	cm.		
1	Inner Fuel Region	39.624	15.600	39.624	15.600	80.010	31.500	81.010	31.500	7.84×10^6	27.867	--	--	4	6	100,000	55,555
2	Center Fuel Region	56.007	22.050	16.383	6.490	80.010	31.500	81.010	31.500	7.84×10^6	27.676	--	--	3	2	100,000	55,555
3	Outer Fuel Region	68.580	27.000	12.573	4.950	80.010	31.500	81.010	31.500	7.87×10^6	27.803	--	--	3	2	100,000	55,555
4	Hot Hydrogen Layer	86.360	34.000	17.780	7.000	86.360	34.000	17.780	7.000	1.68×10^6	51.427	--	--	3	2	100,000	55,555
5	Cool Hydrogen Layer	91.440	36.000	5.080	2.000	91.440	36.000	5.080	2.000	7.57×10^6	26.730	--	--	3	2	5,400	3,000
6	Inner Limer	93.599	36.850	2.159	0.850	93.599	36.850	2.159	0.850	3.48×10^6	12.302	--	1.433	3	2	1,200	667
7	Beryllium Oxide	102.616	40.400	9.017	3.550	102.616	40.400	9.017	3.550	1.64×10^6	57.802	--	1.53×10^6	3	2	2,533	1,405
8	Graphite	124.841	49.150	22.225	8.750	124.841	49.150	22.225	8.750	5.14×10^6	159.945	--	1.18×10^6	3	2	4,067	2,260
9	Beryllium Vessel	126.365	49.750	1.520	0.600	126.365	49.750	1.524	0.600	4.53×10^6	16.002	--	4.36×10^6	3	2	1,200	667
10	Heavy Water	151.638	59.700	25.273	9.750	151.638	59.700	25.273	9.750	9.23×10^6	375.91	--	8.92×10^6	3	2	750	416
11	Tungsten Plumbing	165.100	65.000	13.462	5.300	165.100	65.000	13.462	5.300	6.37×10^6	224.850	--	6.18×10^6	3	2	1,300	555
12	Steel Pressure Shell	188.976	74.400	23.876	9.400	188.976	74.400	23.876	9.400	1.41×10^7	498.224	--	1.30×10^7	3	2	1,000	555

* Total Volumes of regions after penetration by exhaust nozzles and fuel injection duct; volumes shown only when different volumes in preceding columns

TABLE IV

DIMENSIONS OF EXHAUST NOZZLE COMPONENTS AND FUEL INJECTION DUCT USED IN
TWO-DIMENSIONAL CALCULATIONS FOR REFERENCE DESIGN ENGINES WITH NOZZLES

Geometry Shown in Fig. 4 and 5
Composition of Regions Given in Table V

Region Description	No.	Radial Thickness of Region		Axial Thickness of Region		Volume of Region		No. of Radial Mesh Points	No. of Axial Mesh Points	Temperature	
		cm	in.	cm	in.	cu. in.	ft. ³			P	K
Nozzle Approach	13	12.700	5.000	73.660	29.000	4.703 x 10 ⁵	16.606	6	11	20,000	11,150
Nozzle Throat	14	1.422	0.560	23.876	9.400	1.707 x 10 ⁴	0.603	2	3	20,000	11,150
Nozzle Approach Inner Annular Sleeve	15	5.080	2.000	73.660	29.000	1.672 x 10 ⁵	5.904	3	11	2,533	1,405
Nozzle Approach Outer Annular Sleeve	16	5.080	2.000	73.660	29.000	2.090 x 10 ⁵	7.380	3	11	2,533	1,405
Nozzle Throat Inner Annular Sleeve	17	10.719	4.220	23.876	9.400	1.189 x 10 ⁵	4.198	5	3	2,533	1,405
Nozzle Throat Outer Annular Sleeve	18	10.719	4.220	23.876	9.400	1.384 x 10 ⁵	4.887	5	3	2,533	1,405
Fuel Injection Duct	19	1.372	0.540	98.473	38.769	5.823 x 10 ²	0.002	3	13	---	---
Black Absorber Region	20	188.	74.016	3.000	1.1811	3.399 x 10 ⁵	12.002	33	2	---	---

TABLE V

COMPOSITION OF EXHAUST NOZZLE COMPONENTS AND FUEL INJECTION

DUCT USED IN TWO-DIMENSIONAL CALCULATIONS FOR REFERENCE

ENGINE DESIGN WITH NOZZLES

Dimensions of Regions Given in Table IV
 Geometry Shown in Fig. 4 and 5

Region		Volume Fractions				
Description	No.	W-184*	H at 20,000 R	Hf	Be	W-184
Nozzle Approach	13	--	1.0	--	--	--
Nozzle Throat	14	--	1.0	--	--	--
Nozzle Approach Inner Annular Sleeve	15	0.8	--	--	0.150	0.230
Nozzle Approach Outer Annular Sleeve	16	0.8	--	--	0.150	0.230
Nozzle Throat Inner Annular Sleeve	17	0.8	--	--	--	--
Nozzle Throat Outer Annular Sleeve	18	0.8	--	--	--	--
Fuel Injection Duct	19	--	--	0.9	--	--
Black Absorber Region	20	--	--	--	--	--

* Volume Fractions employed for special case in which nozzle approach liner was pure W-184.

TABLE VI

HYDROGEN PARTIAL PRESSURES AND ATOM DENSITIES AT 1000 ATMOSPHERES FOR VARIOUS TEMPERATURES

Partial Pressures And Atom Densities Obtained From Ref. 17

Temperature R	P Atm	P _{H₂} Atm	P _H Atm	P _{H₊} Atm	N _{H₂} $\frac{\text{Atoms}}{\text{cm}^3} \times 10^{-24}$	N _{H+H₊} $\frac{\text{Atoms}}{\text{cm}^3} \times 10^{-24}$	N = N _{H₂} + N _{H+H₊} $\frac{\text{Atoms}}{\text{cm}^3} \times 10^{-24}$
100,000	1000	0	9.2	495.4	0	0.660×10^{-4}	0.660×10^{-4}
20,000	1000	46.7	945.6	3.5	0.610×10^{-4}	0.620×10^{-3}	0.681×10^{-3}
5400	1000	995	5	0	0.481×10^{-2}	0.121×10^{-4}	0.482×10^{-2}

TABLE VII

DENSITIES AND WEIGHTS OF MATERIALS EMPLOYED IN ALL REACTOR CRITICALITY CALCULATIONS

Dimensions of Regions Given in Tables I, III, and IV
 Compositions of Regions Given in Tables II and V
 Geometries Shown in Fig. 2, 3, 4, and 5

Material	Atom Density $\frac{\text{Atoms}}{\text{cm}^3} \times 10^{-24}$	Mass Density**		Total Mass in All Regions in lb			
		gm/cm ³	lb/ft. ³	1-D Spherical Geometry	2-D Reference Geometry, No Nozzle	2-D Reference Engine Design with Nozzles	2-D Reference Engine Design with Modified Nozzle Approach Liner***
Hydrogen, T = 100,000 R ****	0.0000660	0.00011	0.00686	0.2721	0.4082	0.4082	0.4082
Hydrogen, T = 5400 R	0.00482	0.00800	0.4992	8.904	13.35	13.35	13.35
Beryllium Oxide	0.0728	3.020	188.45	6546.0	9814.0	9197.0	9197.0
Beryllium Metal	0.1236	1.850	115.44	1930.0	2895.0	2756.0	3010.0
Pyrolytic Graphite	0.1000	2.000	124.8	99.23	148.8	141.2	141.2
Graphite	0.0802	1.604	100.09	11830.0	17740	16910.0	16910.0
Heavy Water	0.0305	1.010	63.024	14890.0	22340.0	21910.0	21910.0
Hafnium	0.0445	13.200	823.68	--	--	15.25	15.25
* Tungsten-184	0.0632	19.300	1204.3	1218.0	1817.0	14530.0	2100.0
* Natural Tungsten	0.0632	19.300	1204.3	30190.0	45250.0	52720.0	52720.0
Iron	0.0848	7.860	490.46	148400.0	222700.0	208000.0	208000.0
Hydrogen T = 20,000 R	0.000681	0.00113	0.0705	--	--	1.214	1.214

* Natural Tungsten used only in region 11, Tungsten-184 used in all other regions in which Tungsten is specified unless otherwise noted.

** Densities shown correspond to material volume fraction of 1.0; see Tables II and V for actual volume fractions in each region.

*** Cavity liner material in nozzle approach liner replaced by Tungsten-184.

**** Excludes hydrogen in regions 1 to 3.

TABLE VIII

NEUTRON ENERGY GROUP STRUCTURE

Neutron Energy Group	Upper Energy Limit ev	Lower Energy Limit ev	Group Number, Four-Group Structure
1	1.0×10^7	2.865×10^6	1
2	2.865×10^6	1.35×10^6	
3	1.35×10^6	8.21×10^5	
4	8.21×10^5	3.88×10^5	
5	3.88×10^5	1.11×10^5	
6	1.11×10^5	1.50×10^4	
7	1.50×10^4	3.35×10^3	
8	3.35×10^3	5.83×10^2	
9	5.83×10^2	1.01×10^2	2
10	1.01×10^2	29.0	
11	29.0	8.32	3
12	8.32	3.06	
13	3.06	2.38	
14	2.38	1.86	
15	1.86	1.44	
16	1.44	1.125	
17	1.125	0.685	
18	0.685	0.414	
19	0.414	0.3	4
20	0.3	0.2	
21	0.2	0.1	
22	0.1	0.05	
23	0.05	0.015	
24	0.015	0.0	

TABLE IX

ATOMIC HYDROGEN TRANSPORT CROSS SECTIONS

$$\sigma_{tr} = \sigma_s [1 - \overline{\cos\theta}] \Sigma\mu_{1,j} + \sigma_a$$

Neutron Temperature, $T_n = 1405$ K

σ_s Equal Constant 20.0 Barns for All Neutron Energy Groups
($1 - \overline{\cos\theta}$) Obtained From Fig. 8

$\Sigma\mu_{1,j}$ Obtained From Sophist-I (Ref. 20), Calculations
For Up- and Down-Scattering Probabilities

Neutron Energy Group	Atomic Hydrogen Temperature $T_n = 100,000$ R = 55,555 K				Atomic Hydrogen Temperature $T_n = 20,000$ R = 11,150 K			
	σ_a Barns	σ_s Barns	$\Sigma\mu_{1,j}$	$1 - \overline{\cos\theta}$	σ_{tr} Barns	$\Sigma\mu_{1,j}$	$1 - \overline{\cos\theta}$	σ_{tr} Barns
10	0.	20.0	1.045	0.333	6.690	1.000	0.333	6.660
11	0.0139	20.0	1.162	0.505	11.75	1.033	0.382	79.06
12	0.0249	20.0	1.460	0.642	18.75	1.099	0.460	10.14
13	0.03	20.0	1.767	0.724	25.62	1.177	0.541	12.77
14	0.04	20.0	1.937	0.752	29.17	1.226	0.569	13.99
15	0.04	20.0	2.137	0.771	32.99	1.288	0.601	15.52
16	0.05	20.0	2.371	0.794	37.70	1.364	0.631	17.26
17	0.0549	20.0	2.888	0.823	47.59	1.512	0.668	20.25
18	0.0749	20.0	3.562	0.859	61.27	1.814	0.728	26.49
19	0.0892	20.0	4.267	0.882	75.36	2.087	0.770	32.23
20	0.1067	20.0	5.041	0.898	90.64	2.419	0.800	38.81
21	0.1383	20.0	6.495	0.922	119.9	3.046	0.840	51.31
22	0.1938	20.0	9.051	0.948	171.8	4.160	0.882	73.57
23	0.2923	20.0	13.61	0.961	261.9	6.089	0.925	112.94
24	0.5789	20.0	26.92	0.982	529.3	12.147	0.960	233.80

TABLE X

MOLECULAR HYDROGEN TRANSPORT CROSS SECTIONS

$$\sigma_{tr} = \sigma_s [1 - \overline{\cos\theta}] \Sigma_{H,j} + \sigma_a$$

Neutron Temperature, $T_n = 1405$ K

σ_s For Each Neutron Energy Group Obtained From Experimental Measurements For Molecular Hydrogen Reported in Ref. 22
($1 - \overline{\cos\theta}$) Obtained From Fig. 8 For Neutron Energy Groups 14-24, see Text

Concerning Treatment of Groups 10-13
 $\Sigma_{H,j}$ Obtained From Sophist-I (Ref. 20), Calculations
For Up- and Down-Scattering Probabilities

Neutron Energy Group	Hydrogen Temperature $T_H = 20,000$ R = 11,150 K				Hydrogen Temperature $T_H = 5400$ R = 3000 K			
	σ_s Barns	σ_a Barns	$\Sigma_{H,j}$	$1 - \overline{\cos\theta}$	σ_{tr} Barns	$\Sigma_{H,j}$	$1 - \overline{\cos\theta}$	σ_{tr} Barns
10	0.	20.0	1.000	0.333	6.66	1.000	0.333	6.66
11	0.0139	20.0	1.033	0.350	7.25	1.000	0.333	6.66
12	0.0249	20.0	1.099	0.552	12.15	1.031	0.500	10.30
13	0.03	20.2	1.1331	0.600	12.71	1.035	0.535	11.70
14	0.04	20.3	1.160	0.745	17.58	1.041	0.694	14.71
15	0.04	20.4	1.197	0.760	18.60	1.049	0.702	15.06
16	0.05	20.5	1.244	0.774	19.79	1.060	0.710	15.48
17	0.0549	20.9	1.344	0.797	22.44	1.091	0.728	16.65
18	0.0749	21.4	1.554	0.828	27.61	1.138	0.751	18.36
19	0.0892	22.3	1.750	0.850	33.26	1.198	0.777	20.85
20	0.1067	22.8	1.994	0.871	39.71	1.279	0.797	23.35
21	0.1383	24.2	2.464	0.891	53.27	1.451	0.829	29.11
22	0.1938	26.5	3.314	0.924	81.34	1.788	0.869	41.37
23	0.2923	30.0	4.881	0.947	139.0	2.492	0.905	67.95
24	0.5789	45.0	9.521	0.970	416.2	3.618	0.950	154.67

TABLE XI

COMPARISON OF 24-GROUP AND 4-GROUP CALCULATIONS FOR ONE-DIMENSIONAL SPHERICAL CONFIGURATIONS

Geometry, Dimensions, and Compositions of Material
Regions Employed Given in Fig. 2, Tables I and II

U-233 Mass = 35.4 lb in Stepped Concentration Profile (see Fig. 6)
Fluxes Normalized to Produce 1 Neutron/Sec in Fuel Regions

Quantities Compared	4-Group Calculation	24-Group Calculation	Quantities Compared	4-Group Calculation	24-Group Calculation
Effective Multiplication Factor, k_{eff}	0.9857	0.9786	Resonance Neutron Flux in Following Regions (29 to 3.35×10^5 ev)		
Peak Power/Average Power	1.822	1.855	Fuel	27.8	32.69
Fuel Absorption/Fission	0.4457	0.4464	Hydrogen	28.72	33.66
Neutron Absorptions by Following Regions			Reflector-Moderator, Tungsten Plumbing and Pressure Shell	47.50	46.92
Fuel	0.4393	0.4371			
Hydrogen	0.0098	0.0104	Fast Neutron Flux in Following Regions (3.35×10^5 to 10^7 ev)		
Reflector-Moderator, Tungsten Plumbing and Pressure Shell	0.5501	0.5623	Fuel	79.01	102.2
Total Absorptions	0.9992	1.0098	Hydrogen	80.48	104.6
Net Neutron Leakage From Following Regions			Reflector-Moderator, Tungsten Plumbing and Pressure Shell	77.47	75.97
Fuel	+0.5606	+0.5629			
Hydrogen	-0.0098	-0.0104	Total Neutron Flux in Following Regions (0 to 10^7 ev)		
Reflector-Moderator, Tungsten Plumbing and Pressure Shell	-0.5501	-0.5623	Fuel	193.10	219.05
Total Net Neutron Leakage	+0.0007	-0.0098	Hydrogen	204.10	232.00
Thermal Neutron Flux in Following Regions (0 to 29 ev)			Reflector-Moderator, Tungsten Plumbing and Pressure Shell	624.00	566.70
Fuel	86.21	84.16			
Hydrogen	94.94	93.78	Fission Neutron Production Fraction in Fuel Region		
Reflector-Moderator, Tungsten Plumbing and Pressure Shell	479.00	446.80	Inner Fuel Region	0.5992	0.6009
			Center Fuel Region	0.3049	0.3040
			Outer Fuel Region	0.0959	0.0951

TABLE XII

EFFECT OF SUBSTITUTION OF URANIUM-235 OR PLUTONIUM-239 FOR URANIUM-233 ON
CRITICAL MASS IN THE ONE-DIMENSIONAL SPHERICAL CONFIGURATION

Geometry of Spherical Configuration Shown in Fig. 2
Dimensions and Compositons of Material Regions Used
in Spherical Configuration Given in Tables I and II
Calculations Performed Using 24-Group Cross Sections

<u>Nuclear Fuel</u>	<u>Critical Mass</u>	
	<u>M_c</u>	<u>lb</u>
U-233		36.9
U-235		120.0
Pu-239		149.5

TABLE XIII

COMPARISON OF U-233 CRITICAL MASSES FROM REFERENCE 25 AND FROM PRESENT STUDIES

-Studies of Ref. 25 Used One-Dimensional Diffusion Theory, 18 Neutron Energy Groups With Up and Down-Scattering Within 14 of the 18 Groups.

-Present Studies Used One-Dimensional Diffusion Theory, 14 Neutron Energy Groups With Down-Scattering Only - Thermal Group Cross Sections Averaged From Results of 24-Group Calculations For The Same Configuration.

-Geometry, Dimensions, and Compositions of Material Regions Employed In Present Studies Shown In Fig. 2 and Tables I and II.

Source of Data	Gas Pressure In Regions 1 to 5 Atm	Gas Temperature In Regions 1 to 4	Moderator Densities In Regions 7, 8 and 10 lb/ft ³			Thickness of Cold Hydrogen Layer, Region 5 In	Volume Fraction of W-184 In Regions 6, 7, 8, and 10				Critical Mass of U-233 In Steepest Configuration M ₀ , lb
			7	8	10		6	7	8	10	
Ref. 25	500	36,000	188.5	115.0	68.4	0	0	0	0	0	12.3
Present Studies	500	100,000	188.5	115.0	68.4	0	0	0	0	0	16.4
	1000	100,000	188.5	115.0	68.4	0	0	0	0	0	17.3
	1000	100,000	169.5	92.8	59.7	0	0	0	0	0	22.7
	1000	100,000	169.5	92.8	59.7	2.00	0	0	0	0	20.7
	1000	100,000	169.5	92.8	59.7	2.00	.054	0	0	0	33.6
	1000	100,000	169.5	92.8	59.7	2.00	.054	.00076	0	0	34.2
	1000	100,000	169.5	92.8	59.7	2.00	.054	.00076	.00056	0	35.9
	1000	100,000	169.5	92.8	59.7	2.00	.054	.00076	.00056	.00215	36.8

TABLE XIV

COMPARISON OF NEUTRON ABSORPTIONS BY REGIONS FOR ONE-DIMENSIONAL SPHERICAL CONFIGURATION AND TWO-DIMENSIONAL CYLINDRICAL CONFIGURATION WITH NO NOZZLE

Geometry and Dimensions of Spherical Configuratin Given in Fig. 2 and Table I.
 Geometry and Dimensions of Cylindrical Configuration Given in Fig. 3 and Table III.
 Composition of Material Regions for Both Geometries Given in Table II.

Region		Total Absorptions Per Region	
Description	No.	Spherical Configuration	Cylindrical Configuration
Inner Fuel Region	1	0.26290	0.27091
Center Fuel Region	2	0.13410	0.13390
Outer Fuel Region	3	0.04229	0.04181
Hot Hydrogen Layer	4	0.00033	0.00040
Cool Hydrogen Layer	5	0.00976	0.01222
Inner Liner	6	0.05302	0.08076
Beryllium Oxide	7	-0.00836	-0.00055
Graphite	8	0.02802	0.02985
Beryllim Vessel	9	0.00392	0.00418
Heavy Water	10	0.02889	0.02797
Tungsten Plumbing	11	0.42710	0.37996
Steel Pressure Shell	12	0.01764	0.01857
TOTAL		0.99761	0.99998

Ratios of Region Absorptions	Spherical Configuration	Cylindrical Configuration
<u>Fuel Absorptions (Reg. 1, 2, and 3)</u>	<u>0.43929</u>	<u>0.44662</u>
<u>Moderator Absorptions (Reg. 4-10)</u>	<u>0.11558</u> = 3.8007	<u>0.15483</u> = 2.8846
<u>Tungsten Plumbing and Steel Pressure Shell Absorptions (Reg. 11 and 12)</u>	<u>0.44474</u>	<u>0.39853</u>
<u>Moderator Absorptions (Ref. 4-10)</u>	<u>0.11558</u> = 3.8479	<u>0.15483</u> = 2.5740
<u>Inner Liner Absorptions (Reg. 6)</u>	<u>0.05302</u>	<u>0.08076</u>
<u>Moderator Absorptions (Reg. 4-10)</u>	<u>0.11558</u> = 0.4587	<u>0.15483</u> = 0.5216

TABLE XV

SUMMARY OF RESULTS OF TWO-DIMENSIONAL CALCULATIONS

Case	Nozzle Employed	Fuel Injection Duct Employed	Nozzle Throat		Weight of W-184 In Nozzle Approach Liner, lb	Total Weight of W-184 Employed In Moderator Regions, lb	Critical Mass of U-233 lb
1	No	No	--	--	--	1817	35.7
2	Yes	Yes	1.422	0.56	12,820	14,530	60.9
3	Yes	Yes	2.844	1.12	12,820	14,530	60.95
4	Yes	Yes	4.266	1.68	12,820	14,530	60.96
5	Yes	Yes	1.422	0.56	369	2100	50.1
6	Yes	No	1.422	0.56	369	2100	46.3 *

* Estimated from Table II of Ref. 16

TABLE XVI

SUMMARY OF THE EFFECT ON U-233 CRITICAL MASS RESULTING FROM CHANGES IN THE WEIGHTS
OF MODERATOR, PROPELLANT, AND STRUCTURAL MATERIALS AND CHANGES IN
DIMENSIONS OF FUEL, HYDROGEN, AND MODERATOR REGIONS

Type of Calculation	Material	Mc, lb	$\frac{\Delta M_c / M_c}{\Delta M_k}, \text{lb}^{-1}$	$\frac{\Delta M_c / M_c}{\Delta R}, \text{cm}^{-1}$	Comments
1-D, 14-Group Neutron Slowing Down	BeO	36.8	-1.52×10^{-4}	-	Fig. 14
	C	36.8	-6.96×10^{-5}	-	Fig. 15
	D ₂ O	36.8	-3.04×10^{-5}	-1.60×10^{-2}	Based on change in void fraction, Fig. 16.
	D ₂ O	36.8	-2.72×10^{-5}	-	Based on change in D ₂ O region thickness. Fig. 19
	Total Moderator Mass, BeO, C, D ₂ O	36.8	-8.52×10^{-5}	-	Fig. 17
	W-184	36.8	$+7.12 \times 10^{-4}$	-	Based on change in W-184 density in cavity Inner Liner Region, Fig. 18.
	W-Nat	36.8	$+5.34 \times 10^{-3}$	-	Based on change in W-184 enrichment in all regions in which employed, Fig. 20.
1-D, 24-Group, Up-Scattering	He	37.4	-1.66×10^{-3}	-2.75×10^{-2}	Based on change in cool He layer thickness with compensating change in adjacent hot hydrogen region thickness, Fig. 13.
	Fuel	37.4	-	-5.07×10^{-3}	Based on change in fuel region radius with compensating change in adjacent hot hydrogen region thickness, Fig. 12.
2-D, 4-Group	W-184	50.1	$+1.74 \times 10^{-5}$	-	Based on removal of W-184 from exhaust Nozzle approach liner, Fig. 24.
	Total Moderator Mass, BeO, C, D ₂ O	50.1	-1.68×10^{-4}	-	Based on removal of moderator material to create exhaust nozzle approach, Fig. 21 and 24.

LAYOUT DRAWING OF ENGINE DESIGN CONFIGURATION

- DETAILS GIVEN IN REF. 1

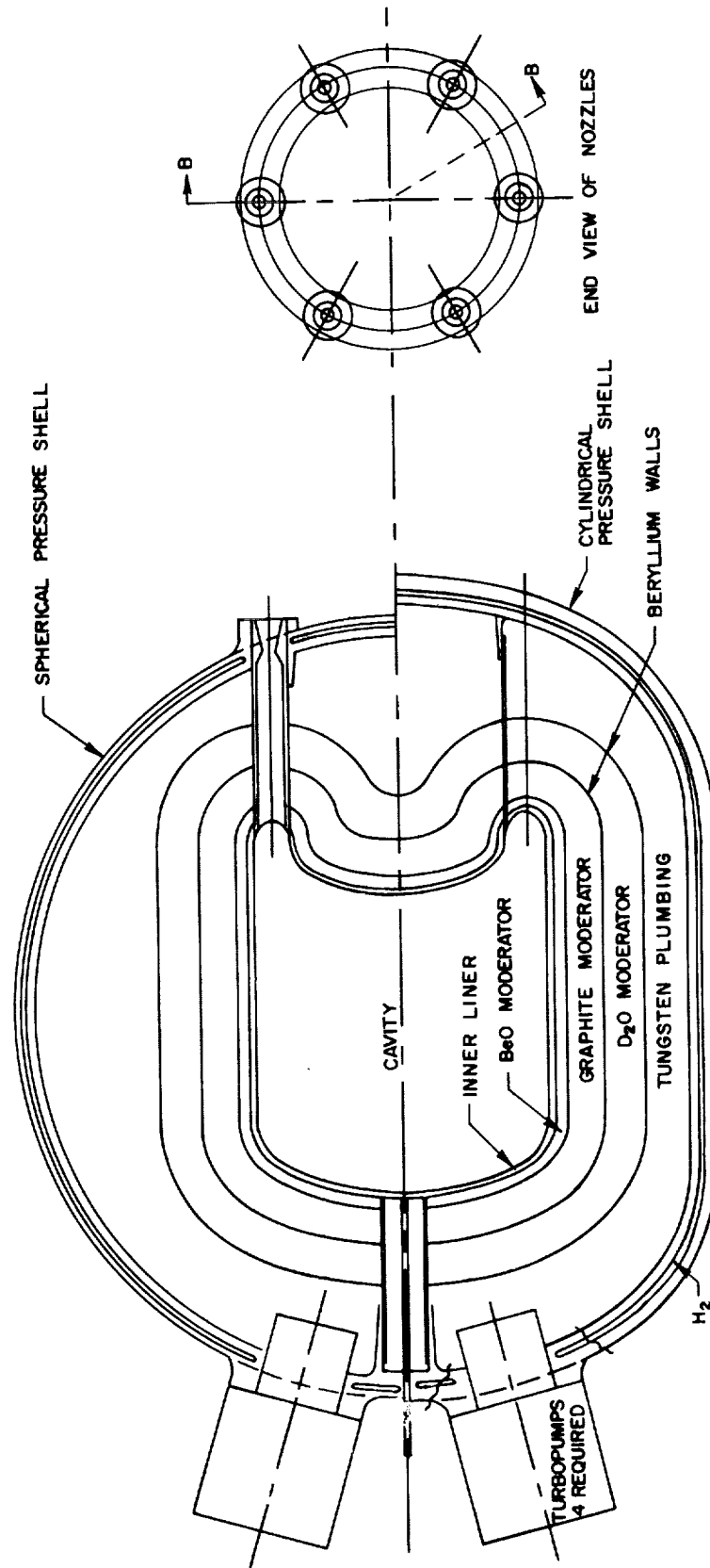


FIG. 1

FIG. 2

BASIC SPHERICAL GEOMETRY USED IN ONE-DIMENSIONAL CALCULATIONS

- CONFIGURATION SPHERICALLY SYMMETRIC
- ALL DIMENSIONS IN CM
- CIRCLED NUMBERS INDICATE REGIONS DESCRIBED IN TABLES II TO IV

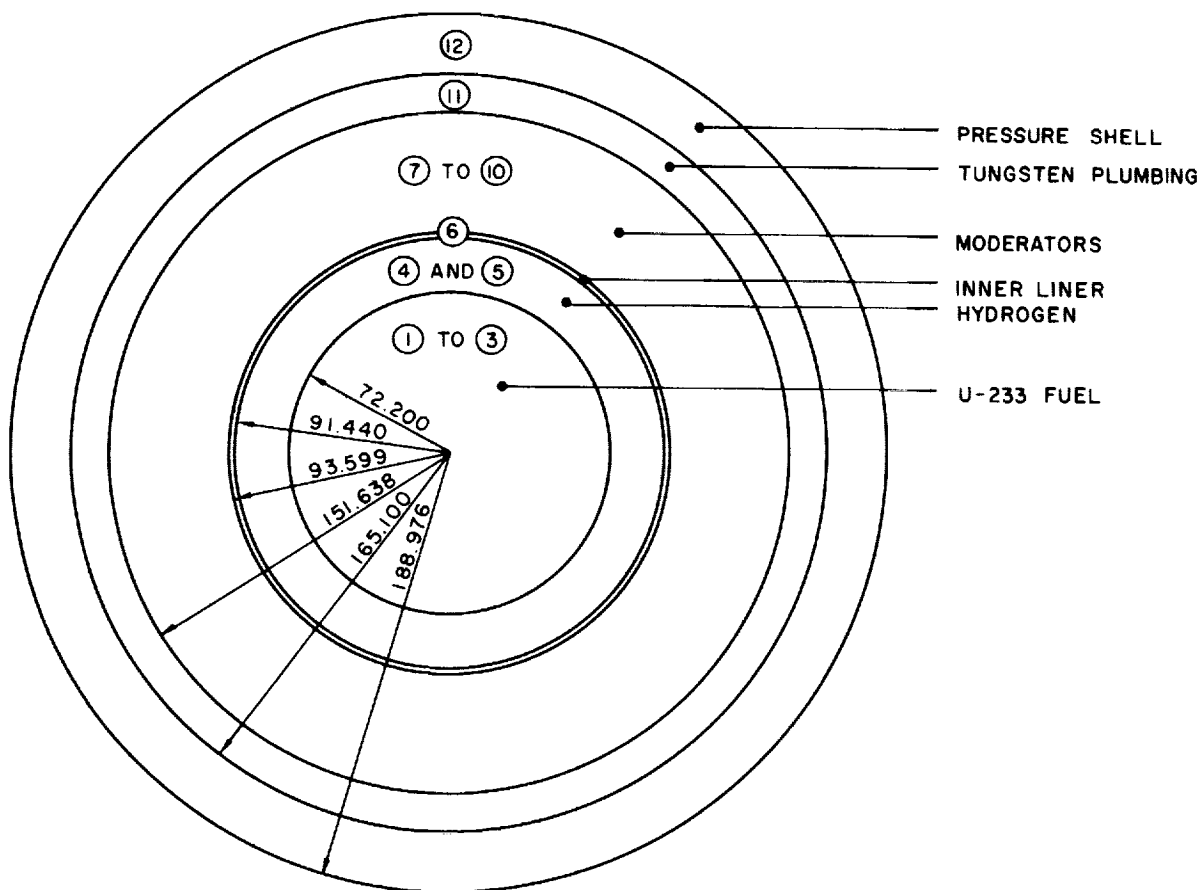


FIG. 3

BASIC CYLINDRICAL GEOMETRY USED IN TWO-DIMENSIONAL CALCULATIONS

- CONFIGURATION SYMMETRICAL ABOUT AXIAL CENTERLINE AND RADIAL MID-PLANE
- ALL DIMENSIONS IN CM
- CIRCLED NUMBERS INDICATE REGIONS DESCRIBED IN TABLES II TO IV

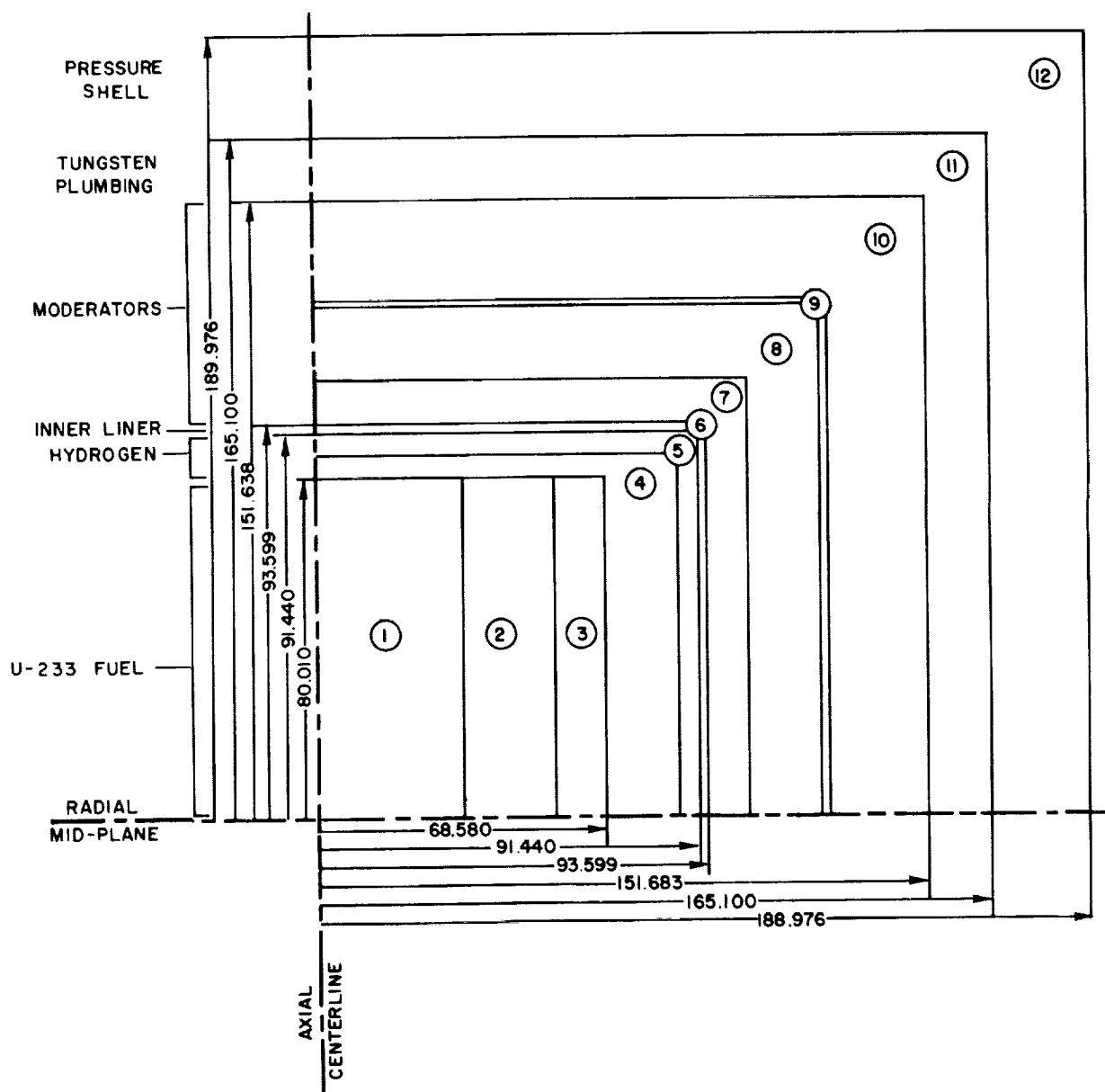


FIG. 4

GEOMETRY OF EXHAUST NOZZLE USED IN SOME TWO - DIMENSIONAL CALCULATIONS

- CONFIGURATION SYMMETRICAL ABOUT AXIAL CENTERLINE, BUT NOT RADIAL MID-PLANE
- ALL DIMENSIONS IN CM
- SEE FIG. 3 AND TABLES II THROUGH IV FOR DESCRIPTION OF REGION NUMBERS

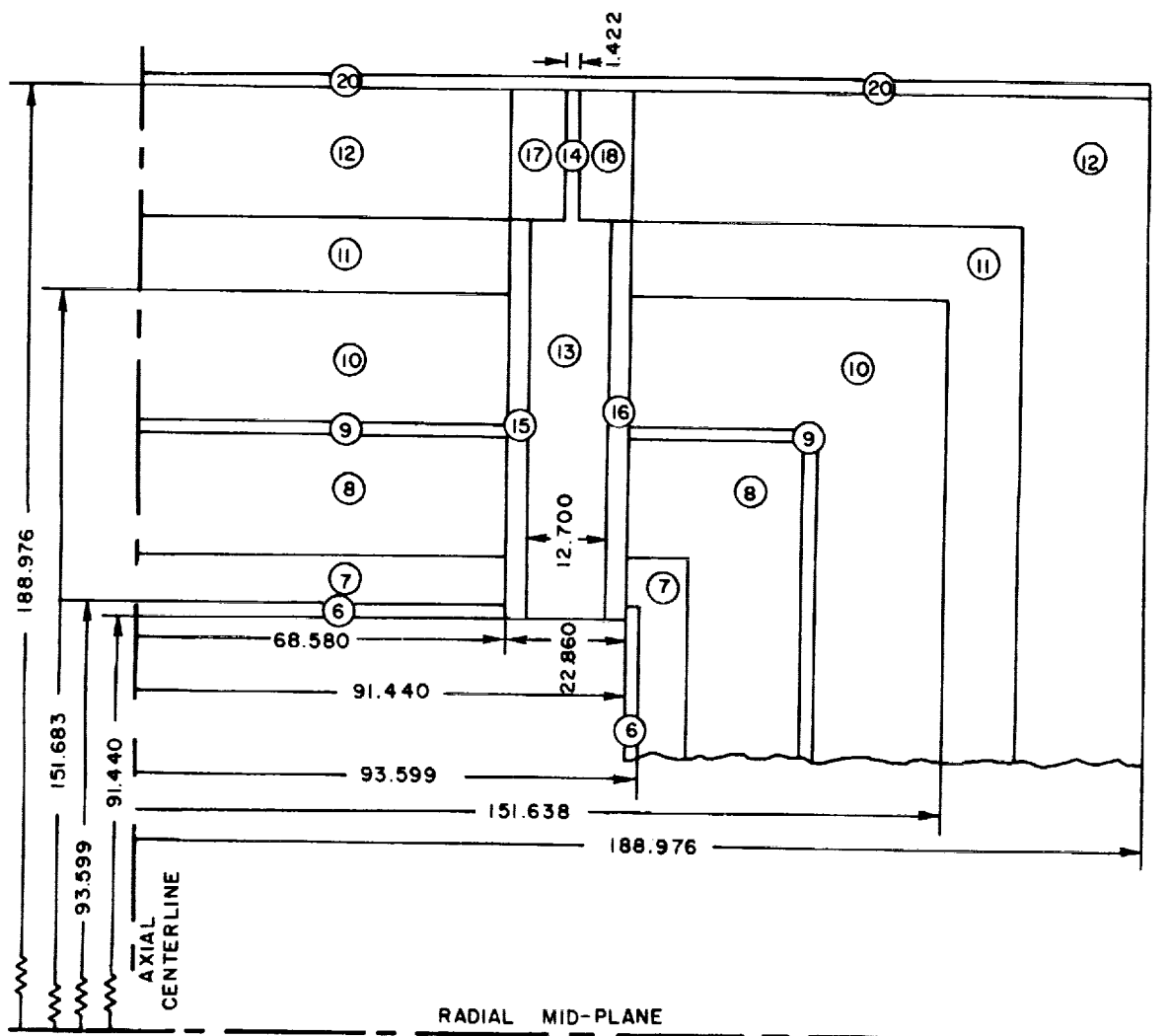


FIG. 5

GEOMETRY OF FUEL-INJECTION DUCT USED IN SOME TWO - DIMENSIONAL CALCULATIONS

- CONFIGURATION SYMMETRICAL ABOUT AXIAL CENTERLINE, BUT NOT RADIAL MID-PLANE
- ALL DIMENSIONS IN CM
- SEE FIG. 3 AND TABLES II TO IV FOR DESCRIPTION OF REGION NUMBERS

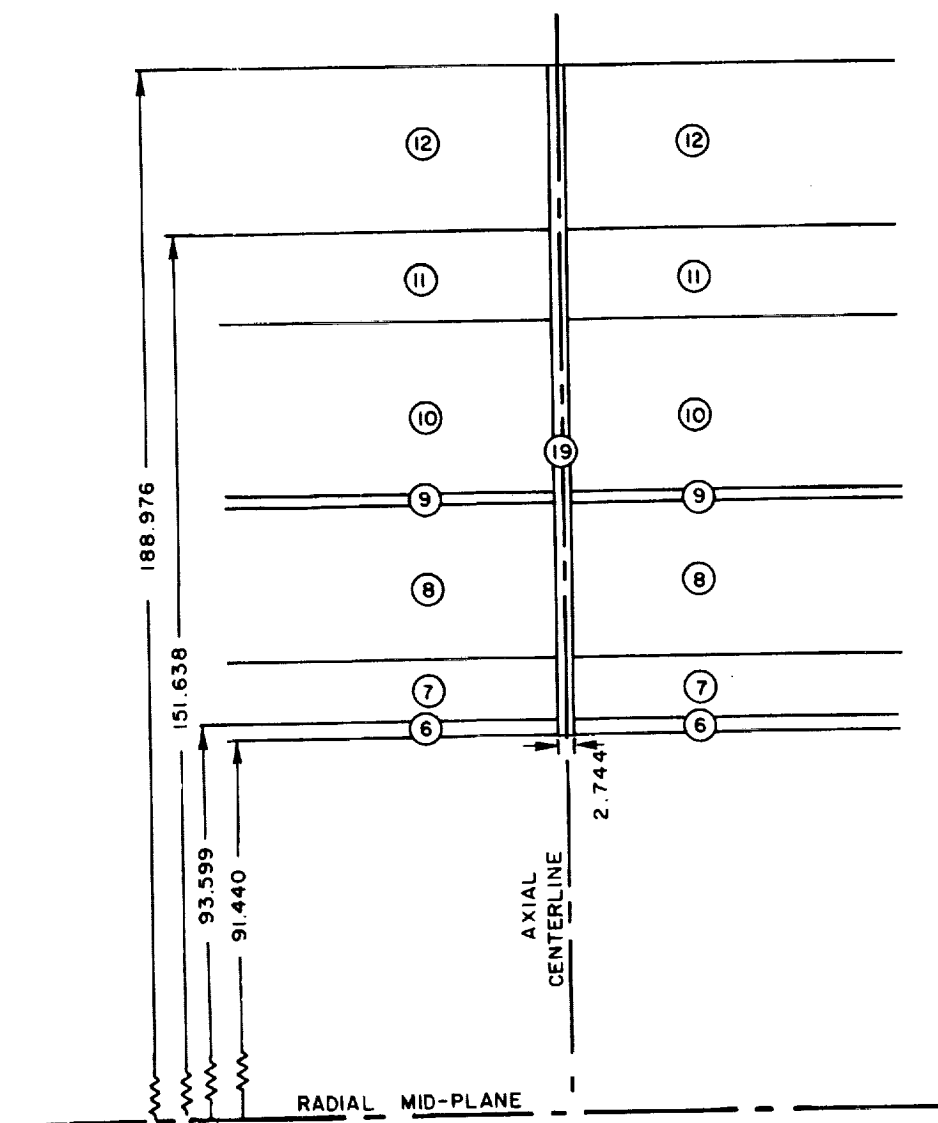


FIG. 6

FUEL CONCENTRATION PROFILES USED IN ONE- AND TWO-DIMENSIONAL CALCULATIONS TO SIMULATE LINEAR VARIATION OF NUCLEAR FUEL DENSITY WITH RADIUS FROM CENTERLINE TO OUTSIDE EDGE OF FUEL

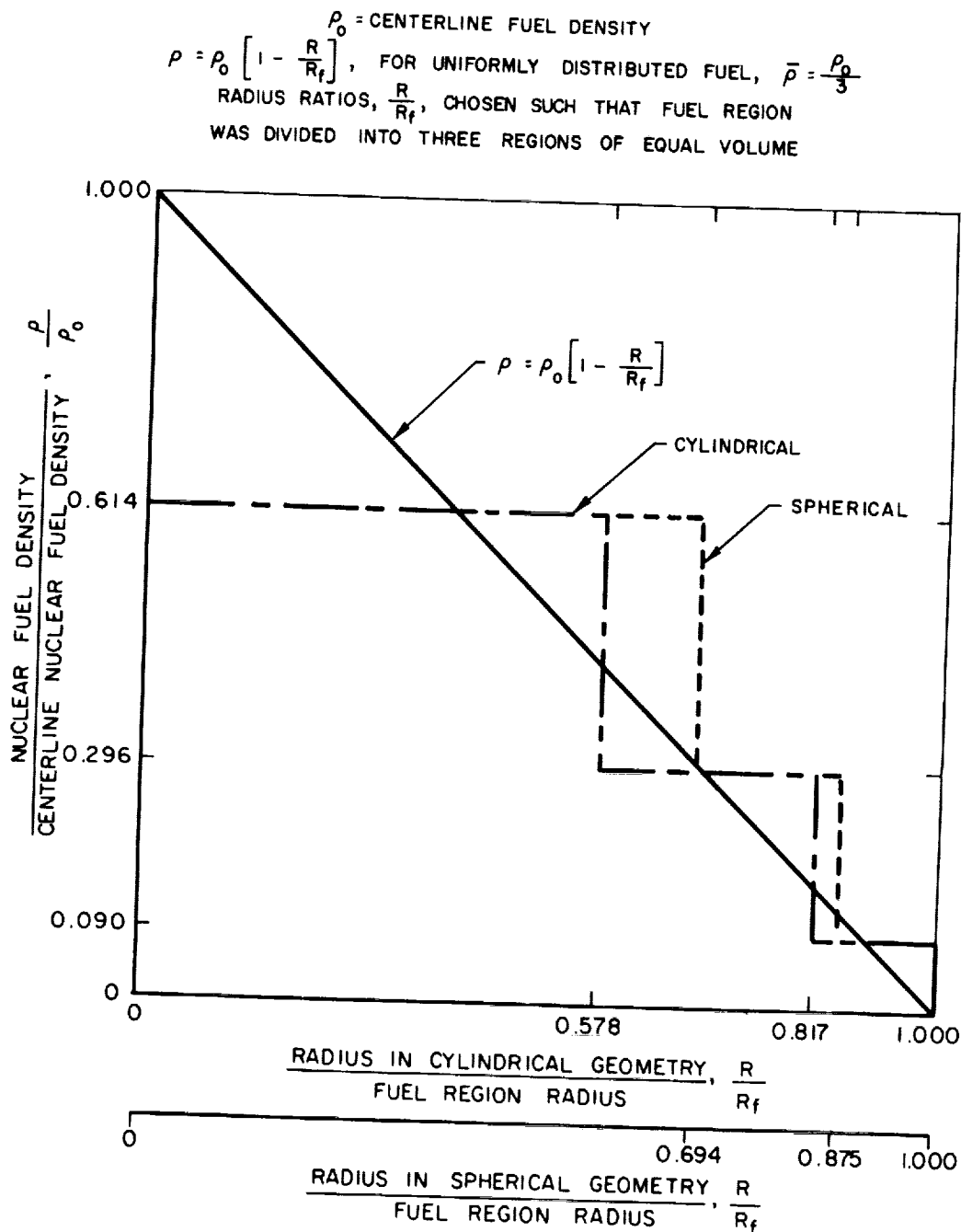


FIG. 7

HYDROGEN AND URANIUM ION DENSITIES FOR FUEL AND HYDROGEN MIXTURE

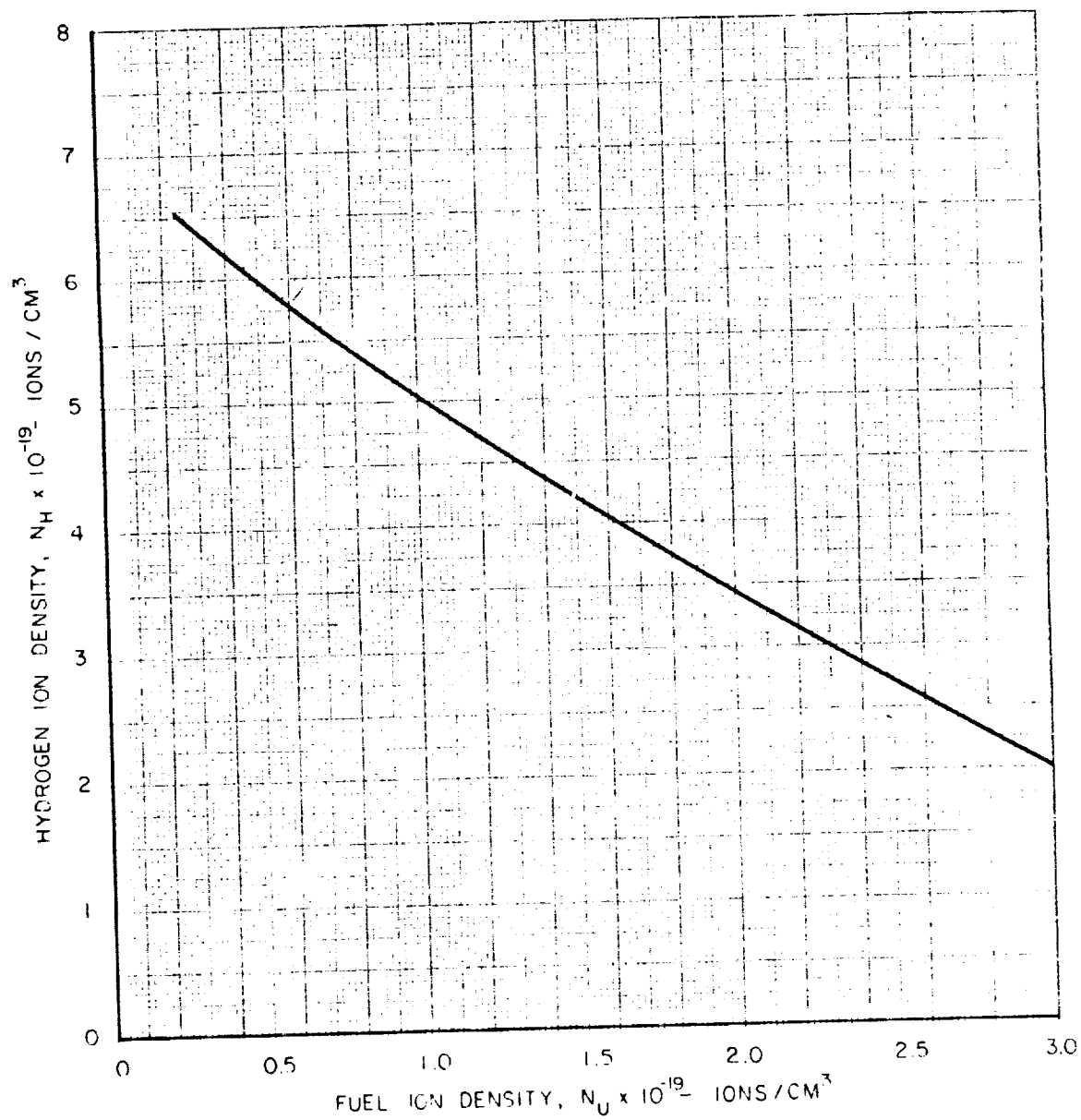
$T = 100,000 \text{ R}$ $P = 1000 \text{ ATM}$

TOTAL PARTICLE DENSITY = $1.32 \times 10^{20} \text{ CM}^{-3}$

NUMBER DENSITY OF HYDROGEN ELECTRONS = NUMBER DENSITY OF HYDROGEN IONS

FUEL APPROXIMATELY TRIPLY IONIZED (NUMBER DENSITY OF FUEL

ELECTRONS $\cong 3$ TIMES NUMBER DENSITY OF FUEL IONS)

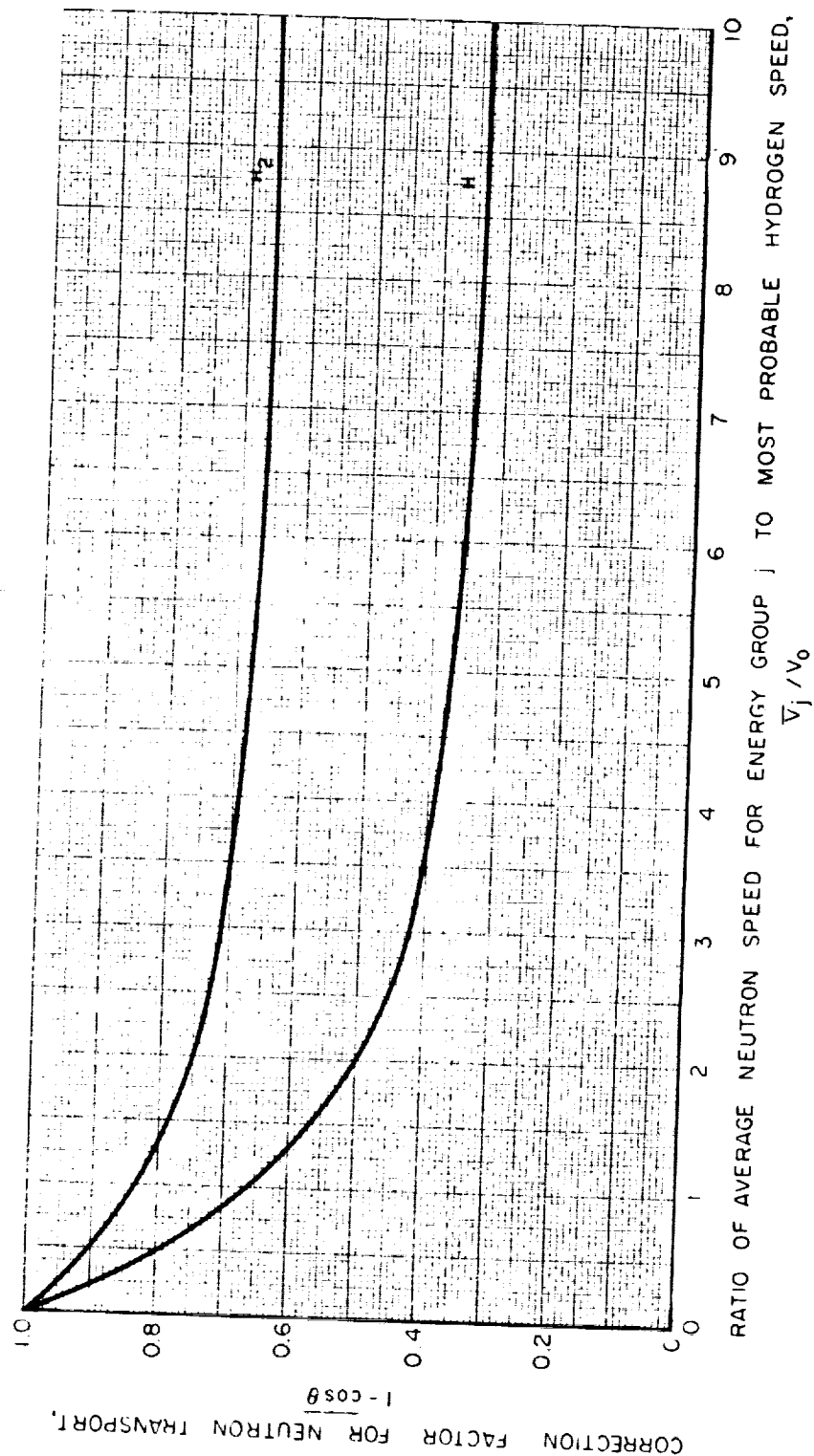


NEUTRON TRANSPORT CORRECTION FOR SCATTERING INTERACTIONS BETWEEN THERMAL NEUTRONS AND ATOMIC AND MOLECULAR HYDROGEN

$$1 - \overline{\cos \theta} = \frac{a_j(v)}{a(v)} \quad \text{FROM FIG. 2, REF 21}$$

$$\bar{v}_j = 138 \times 10^3 \sqrt{E_j} \quad \text{CM/SEC (NEUTRON SPEED FOR ENERGY GROUP } j)$$

$$v_0 = \left[\frac{2kT}{m} \right]^{1/2} \quad \text{CM/SEC (HYDROGEN MOST PROBABLE SPEED)}$$



H_2 MICROSCOPIC SCATTERING CROSS SECTION PER ATOM

MEASUREMENTS REPORTED IN REF. 22

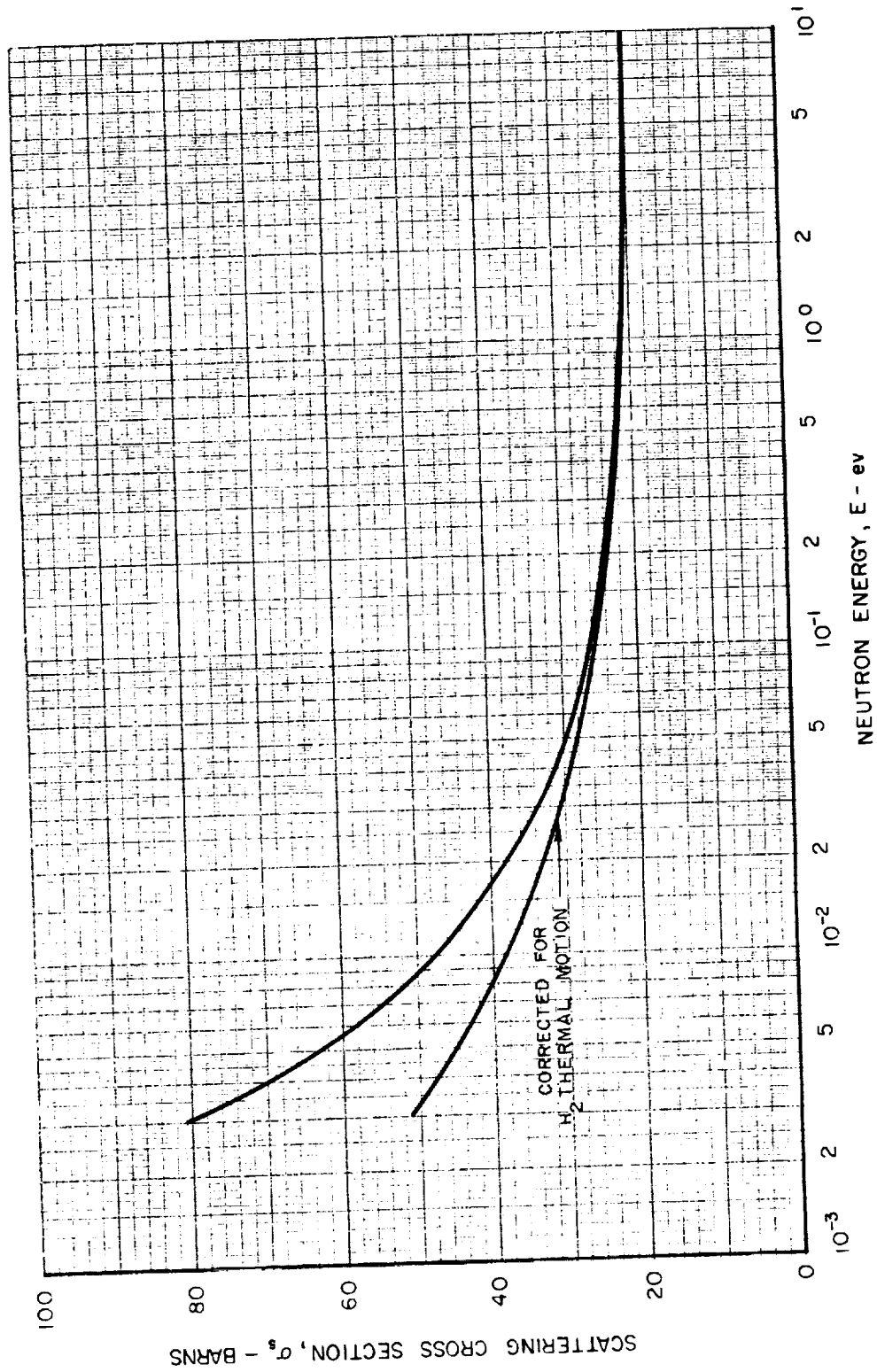


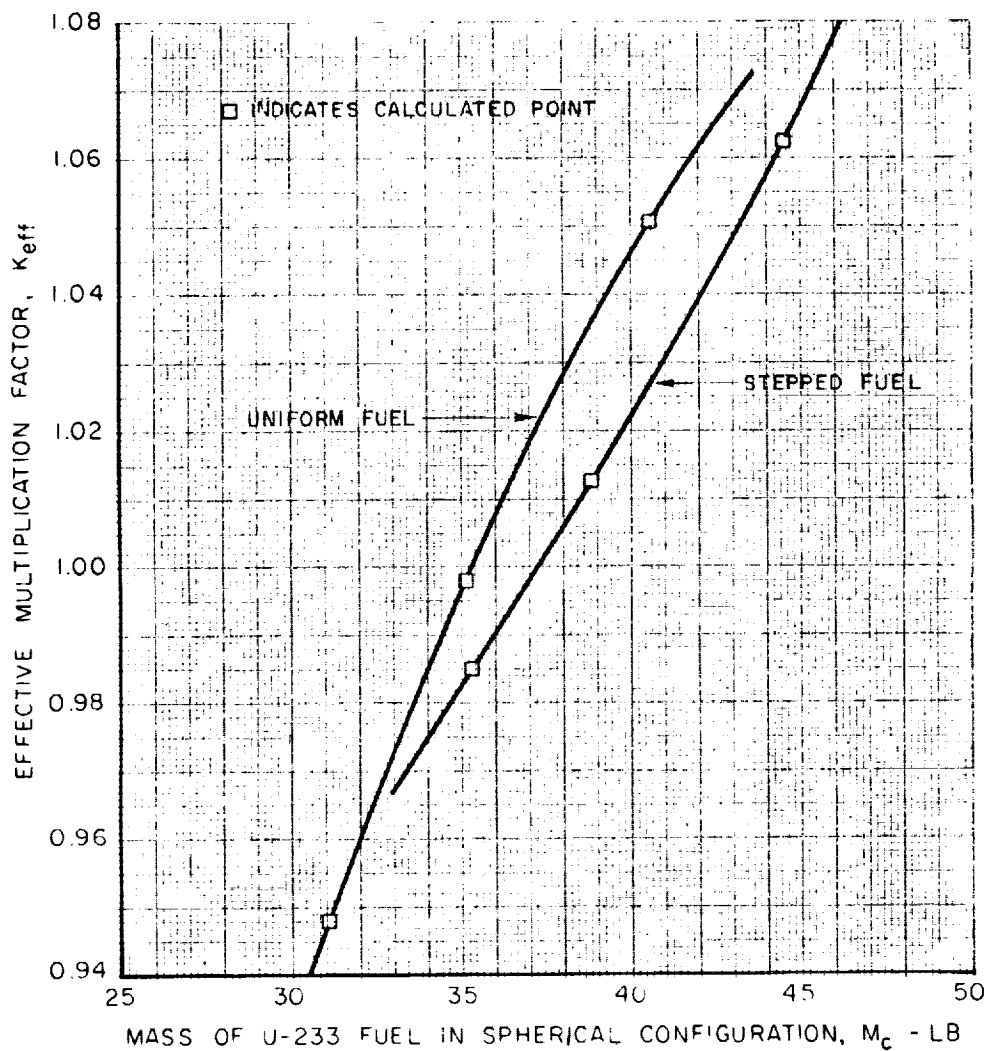
FIG. 9

U-233 CRITICAL MASS DETERMINATION USING 24 - NEUTRON - ENERGY - GROUPS FOR ONE - DIMENSIONAL SPHERICAL GEOMETRY

- DIMENSIONS AND COMPOSITIONS USED IN SPHERICAL CONFIGURATION GIVEN IN TABLES I AND II
- GEOMETRY FOR SPHERICAL CONFIGURATION SHOWN IN FIG. 2

TABLE OF RESULTS

FUEL DENSITY PROFILE	U-233 CRITICAL MASS	$\frac{\Delta K/K}{\Delta M_c/M_c}$
UNIFORM	35.25	0.402
STEPPED	37.25	0.306



NEUTRON FLUX SPECTRA AND INTEGRATED FLUXES FROM 24-NEUTRON-ENERGY- GROUP ONE - DIMENSIONAL CALCULATIONS IN SPHERICAL GEOMETRY

-SPECTRA NORMALIZED SUCH THAT FLUX PEAK = 1 NEUTRON / CM² - SEC - ev
 -INTEGRATED FLUXES NORMALIZED SUCH THAT $\Phi = 1$ NEUTRON / CM² - SEC
 -DIMENSIONS AND COMPOSITIONS USED IN SPHERICAL CONFIGURATION GIVEN IN TABLES I AND II

KEY TO CURVES

LINE	REGION DESCRIPTION	REGION NUMBER	REGION BOUNDARIES - CM
---	CENTER FUEL REGION	2	50.1 - 63.1
---	HOT HYDROGEN	4	72.2 - 86.4
---	COOL HYDROGEN LAYER	5	86.4 - 91.4
---	BERYLLIUM OXIDE	7	93.6 - 102.3
---	GRAPHITE	8	102.3 - 124.8
---	HEAVY WATER	10	126.4 - 151.6

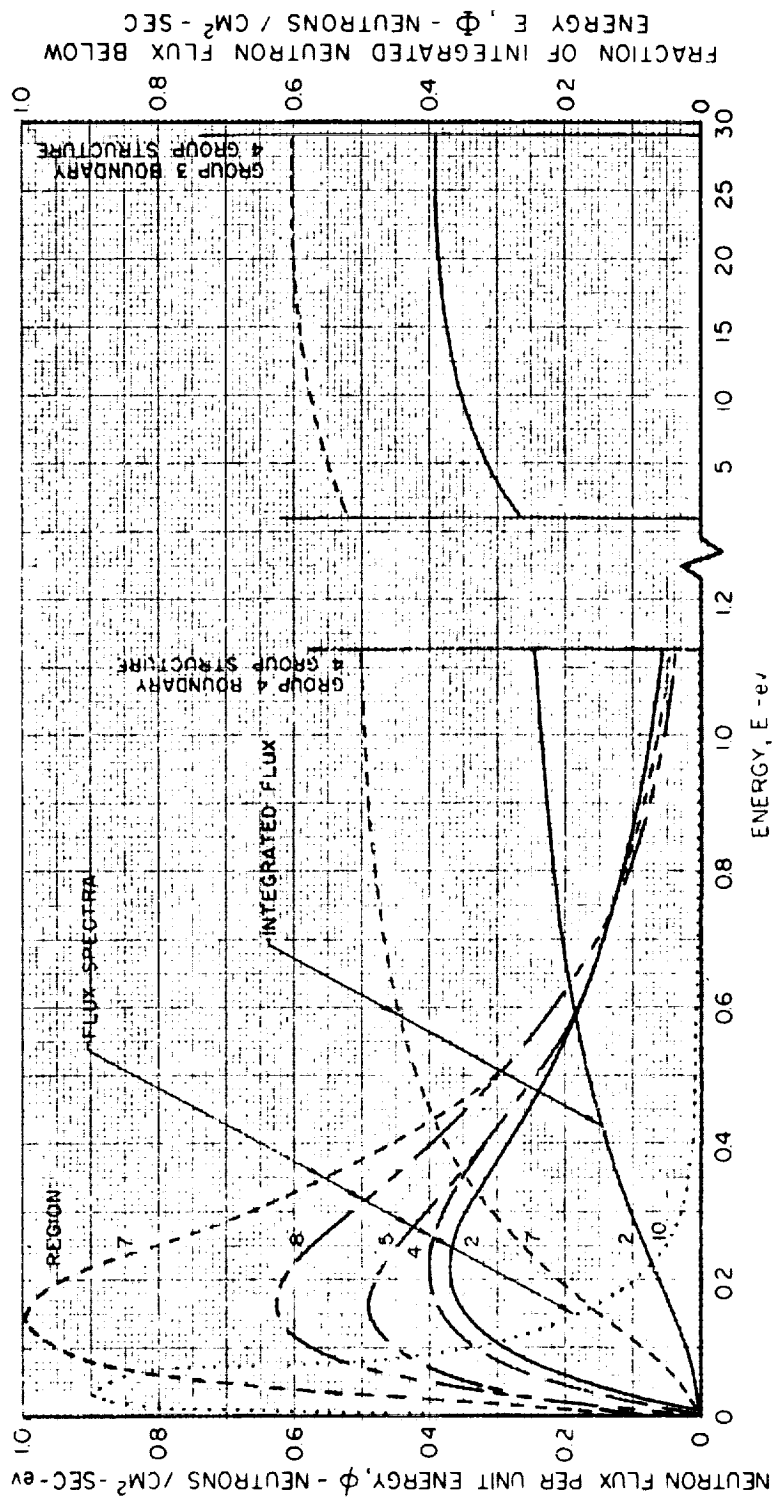


FIG. 11

FIG. 12

EFFECT OF FUEL VOLUME VARIATION ON U-233 CRITICAL MASS FROM ONE-DIMENSIONAL CALCULATIONS USING 24-NEUTRON-ENERGY GROUPS

- DIMENSIONS AND COMPOSITIONS FOR BASIC SPHERICAL CONFIGURATION GIVEN IN TABLES I AND II
- THICKNESS OF HOT HYDROGEN REGION SURROUNDING FUEL (REGION 4, SEE FIG. 2) MODIFIED WITH EACH CHANGE IN FUEL REGION RADIUS

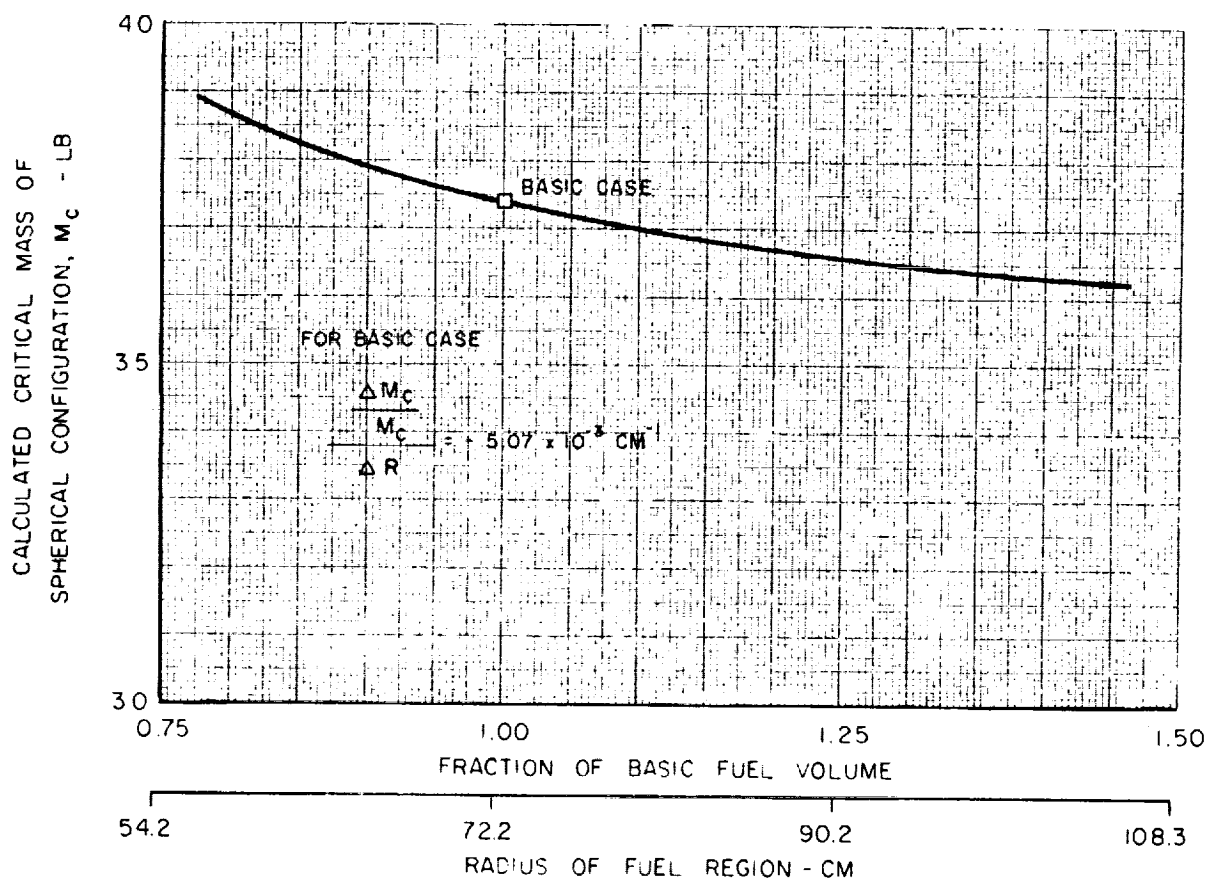


FIG. 13

**EFFECT OF VARIATION OF THICKNESS OF COOL HYDROGEN
LAYER NEAR CAVITY WALL ON U-233 CRITICAL
MASS FROM ONE-DIMENSIONAL CALCULATIONS
USING 24-NEUTRON-ENERGY GROUPS**

- DIMENSIONS AND COMPOSITIONS FOR BASIC SPHERICAL CONFIGURATION GIVEN IN TABLES I AND II
- THICKNESS OF HOT HYDROGEN REGION SURROUNDING FUEL (REGION 4; SEE FIG 2) MODIFIED WITH EACH CHANGE IN THICKNESS OF COOL HYDROGEN LAYER (REGION 5; SEE FIG 2)

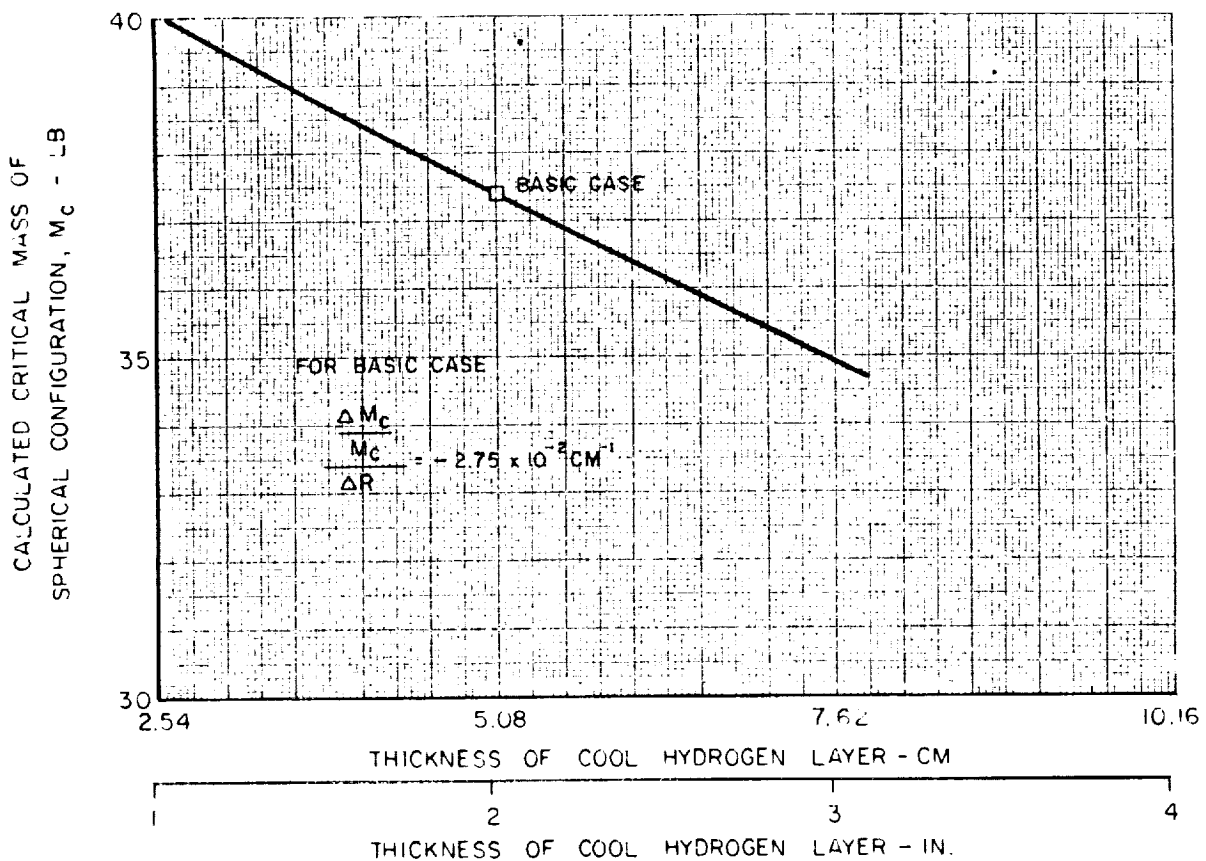
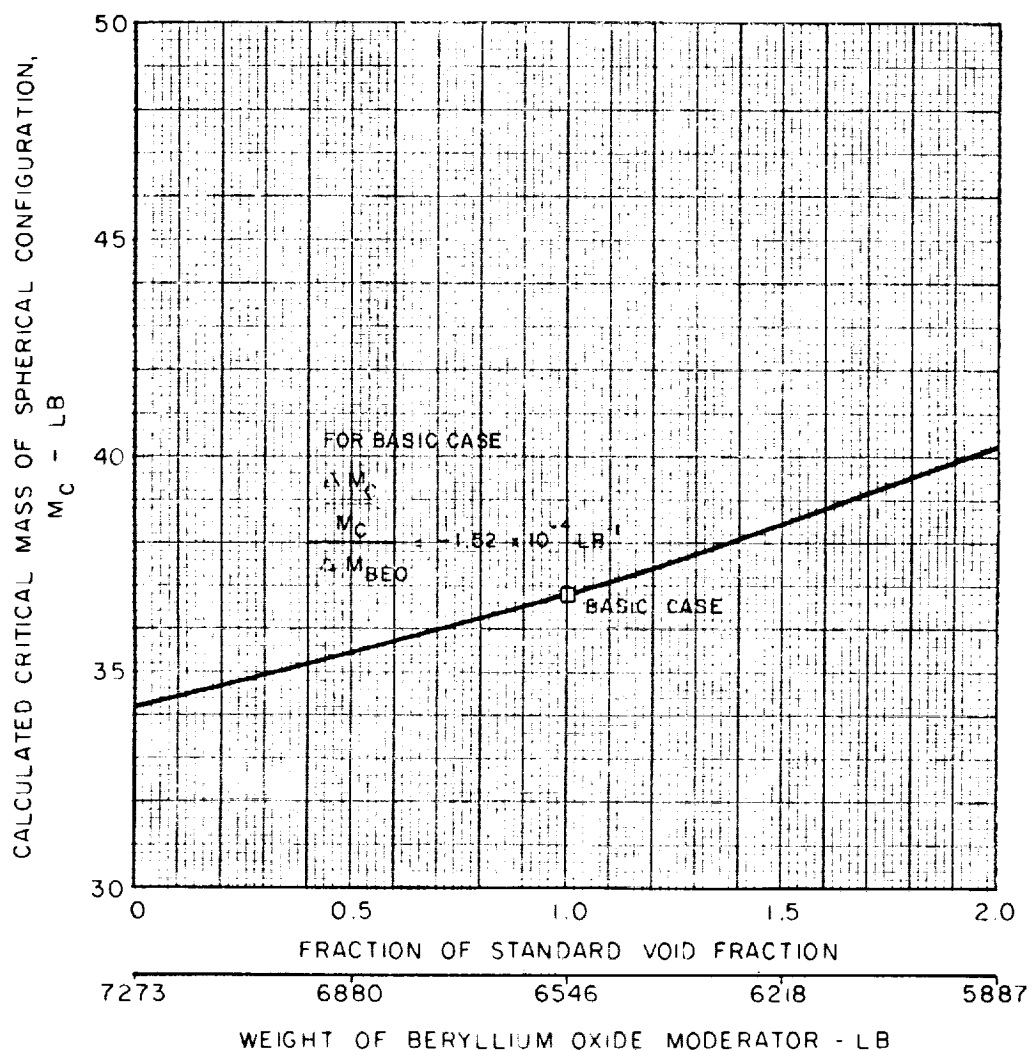


FIG. 14

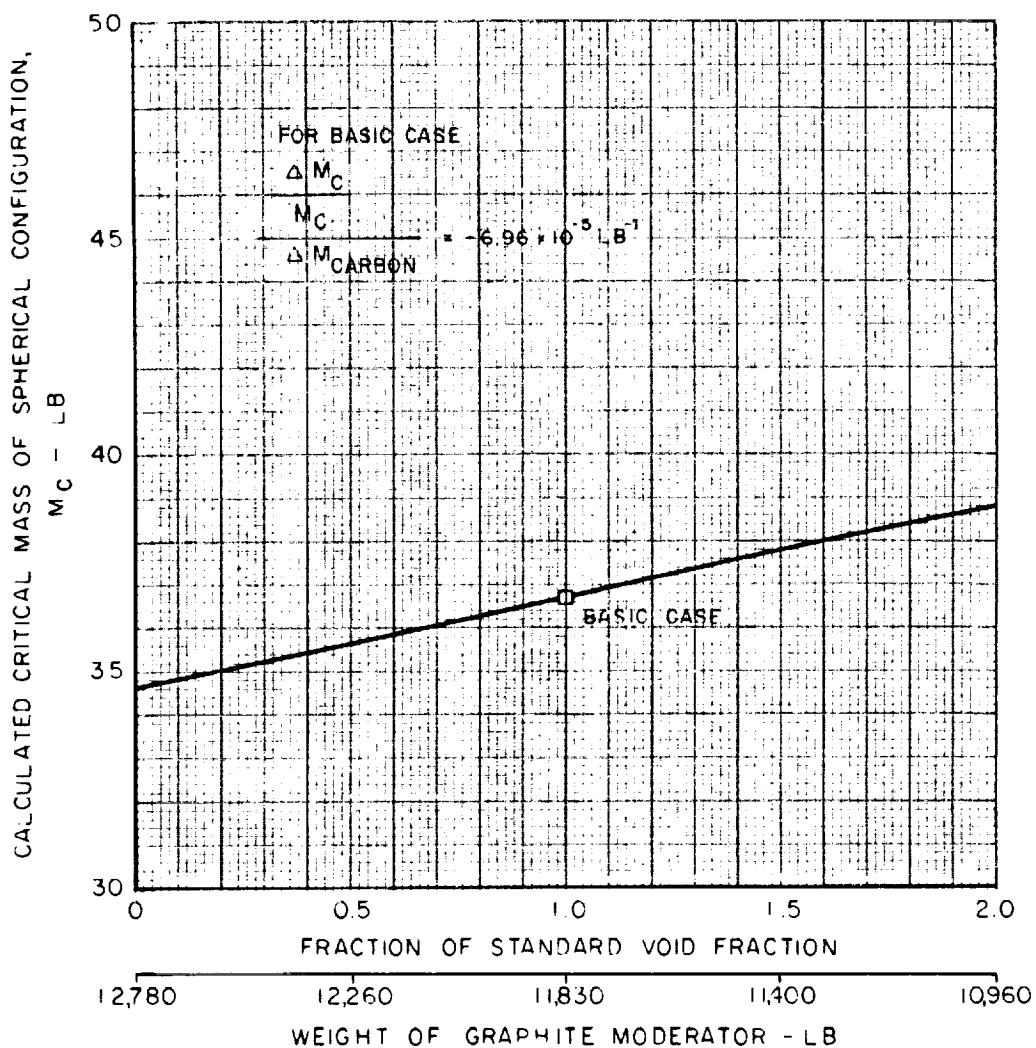
ONE - DIMENSIONAL CALCULATION OF THE EFFECT OF VARIATION OF VOID FRACTION IN BERYLLIUM OXIDE MODERATOR REGION ON U-233 CRITICAL MASS

- CALCULATIONS MADE IN SPHERICAL GEOMETRY WITH UNIFORM FUEL DENSITY PROFILE
- ONE THERMAL NEUTRON ENERGY GROUP USED WITH AVERAGED CROSS SECTIONS FROM 24-NEUTRON-ENERGY-GROUP CALCULATIONS
- STANDARD VOID FRACTION IN BERYLLIUM OXIDE MODERATOR REGION = 0.091



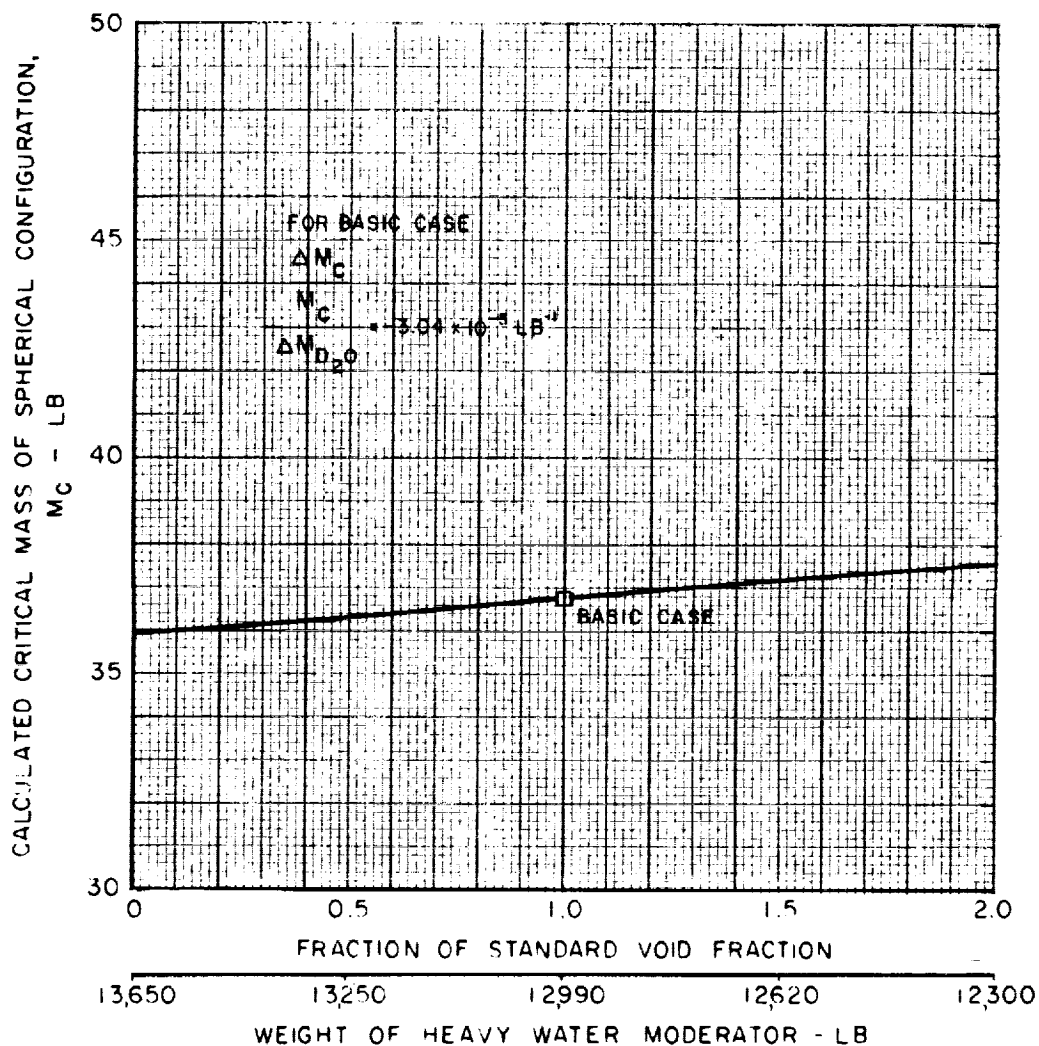
ONE - DIMENSIONAL CALCULATION OF THE EFFECT OF VARIATION OF VOID FRACTION IN GRAPHITE MODERATOR REGION ON U-233 CRITICAL MASS

- CALCULATIONS MADE IN SPHERICAL GEOMETRY WITH UNIFORM FUEL DENSITY PROFILE
- ONE THERMAL NEUTRON ENERGY GROUP USED WITH AVERAGED CROSS SECTIONS FROM 24-NEUTRON-ENERGY-GROUP CALCULATIONS
- STANDARD VOID FRACTION IN GRAPHITE MODERATOR REGION = 0.068



ONE - DIMENSIONAL CALCULATION OF THE EFFECT OF VARIATION OF VOID FRACTION IN HEAVY WATER MODERATOR REGION ON U-233 CRITICAL MASS

- CALCULATIONS MADE IN SPHERICAL GEOMETRY WITH UNIFORM FUEL DENSITY PROFILE
- ONE THERMAL NEUTRON ENERGY GROUP USED WITH AVERAGED CROSS SECTIONS FROM 24-NEUTRON-ENERGY-GROUP CALCULATIONS
- STANDARD VOID FRACTION IN HEAVY WATER MODERATOR REGION = 0.046



ONE-DIMENSIONAL CALCULATION OF THE EFFECT OF VARIATION OF VOID FRACTION IN BERYLLIUM OXIDE, GRAPHITE, AND HEAVY WATER MODERATOR REGIONS ON U-233 CRITICAL MASS

- CALCULATIONS MADE IN SPHERICAL GEOMETRY WITH UNIFORM FUEL DENSITY PROFILE
- ONE THERMAL NEUTRON ENERGY GROUP USED WITH AVERAGED CROSS SECTIONS FROM 24-NEUTRON-ENERGY-GROUP CALCULATIONS
- STANDARD VOID FRACTION IN BERYLLIUM OXIDE REGION = 0.091, GRAPHITE REGION = 0.068, AND HEAVY WATER REGION = 0.046

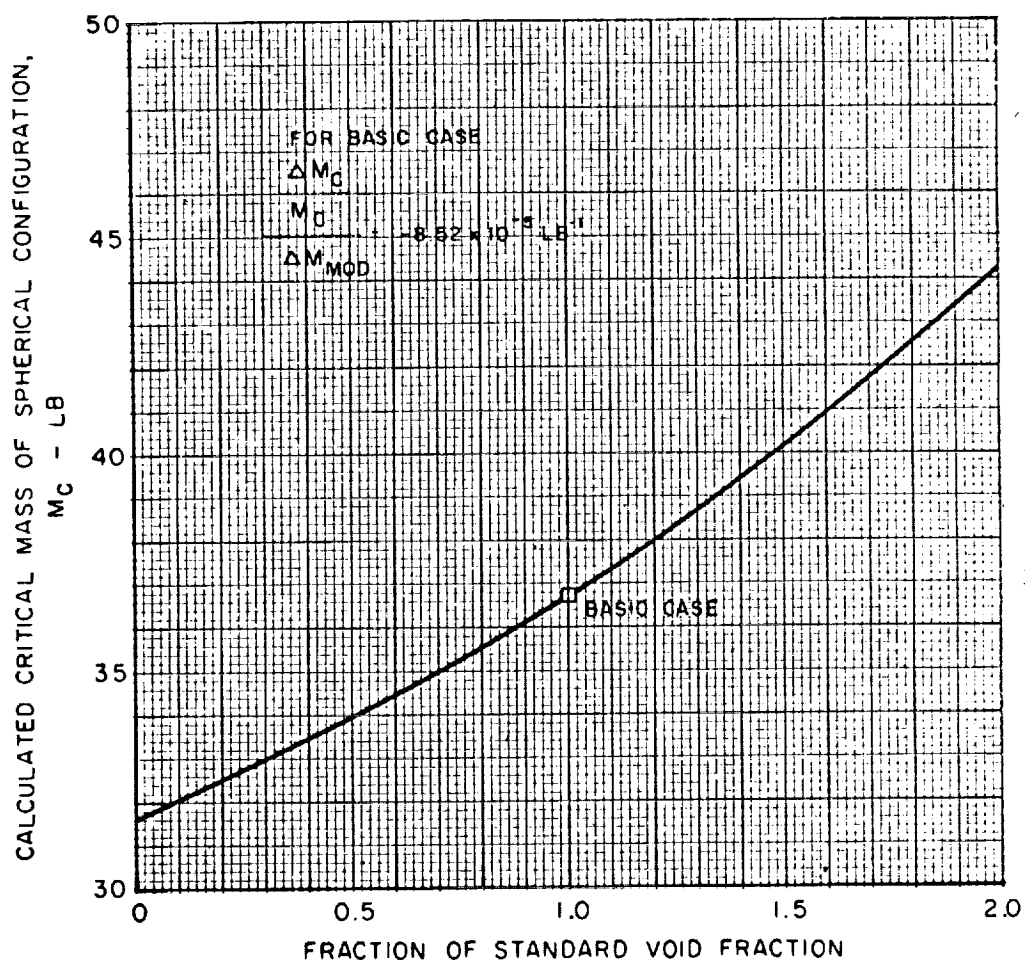


FIG. 18

ONE - DIMENSIONAL CALCULATION OF THE EFFECT OF VARIATION OF DENSITY OF TUNGSTEN-184 IN INNER LINER ON U-233 CRITICAL MASS

- CALCULATIONS MADE IN SPHERICAL GEOMETRY WITH UNIFORM FUEL DENSITY PROFILE
- ONE THERMAL NEUTRON ENERGY GROUP USED WITH AVERAGED CROSS SECTIONS FROM 24-NEUTRON-ENERGY-GROUP CALCULATIONS
- FOR BASIC CASE, INNER LINER THICKNESS = 0.85 IN. = 2.159 CM (SEE TABLE I REGION 6)
- WEIGHT OF TUNGSTEN-184 IN INNER LINER FOR BASIC CASE = 533.6 LB

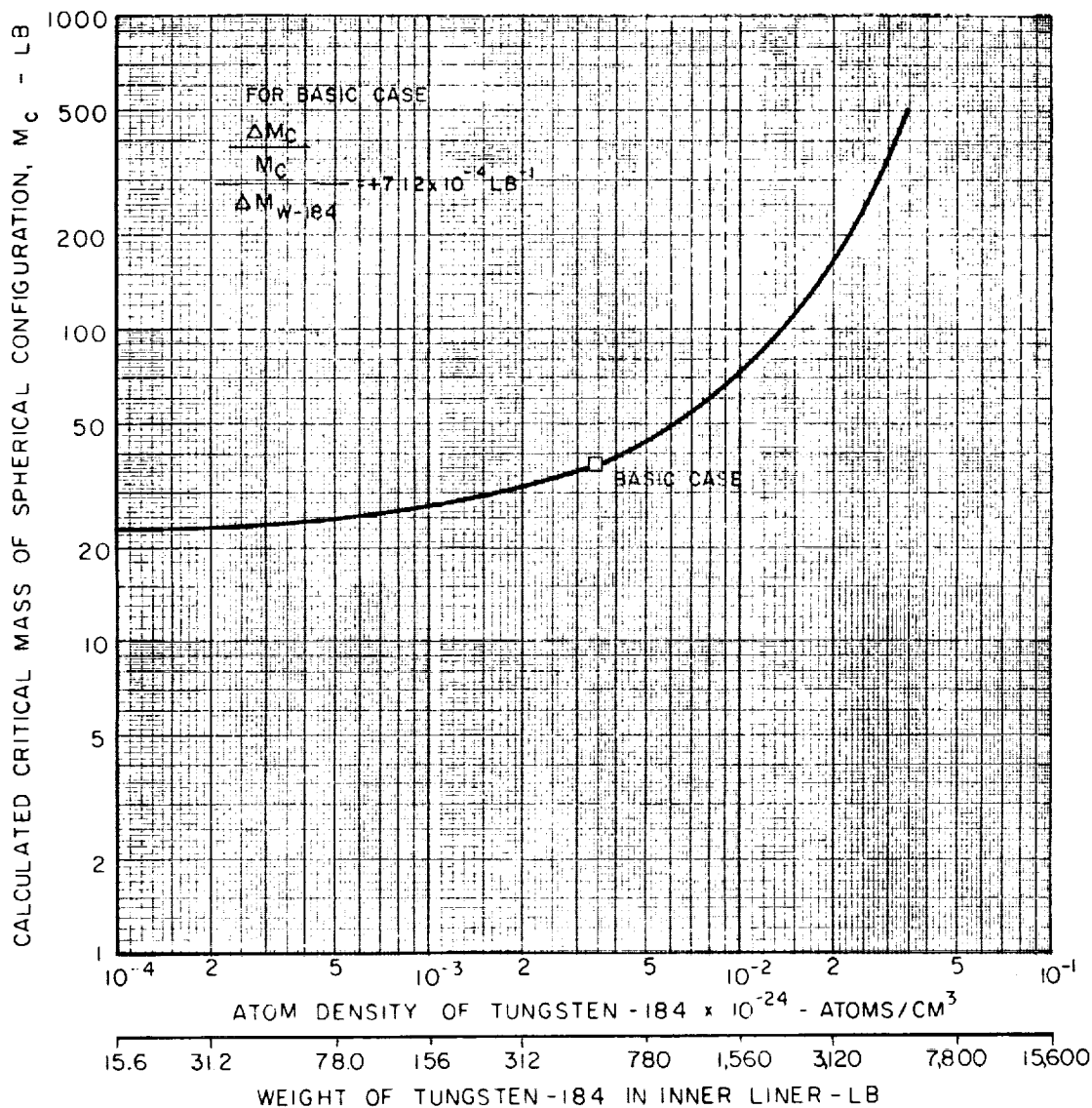


FIG. 19

ONE - DIMENSIONAL CALCULATION OF THE EFFECT OF VARIATION OF HEAVY WATER MODERATOR REGION THICKNESS ON U - 233 CRITICAL MASS

- CALCULATIONS MADE IN SPHERICAL GEOMETRY WITH UNIFORM FUEL DENSITY PROFILE
- ONE THERMAL NEUTRON ENERGY GROUP USED WITH AVERAGED CROSS SECTIONS FROM 24-NEUTRON-ENERGY-GROUP CALCULATIONS

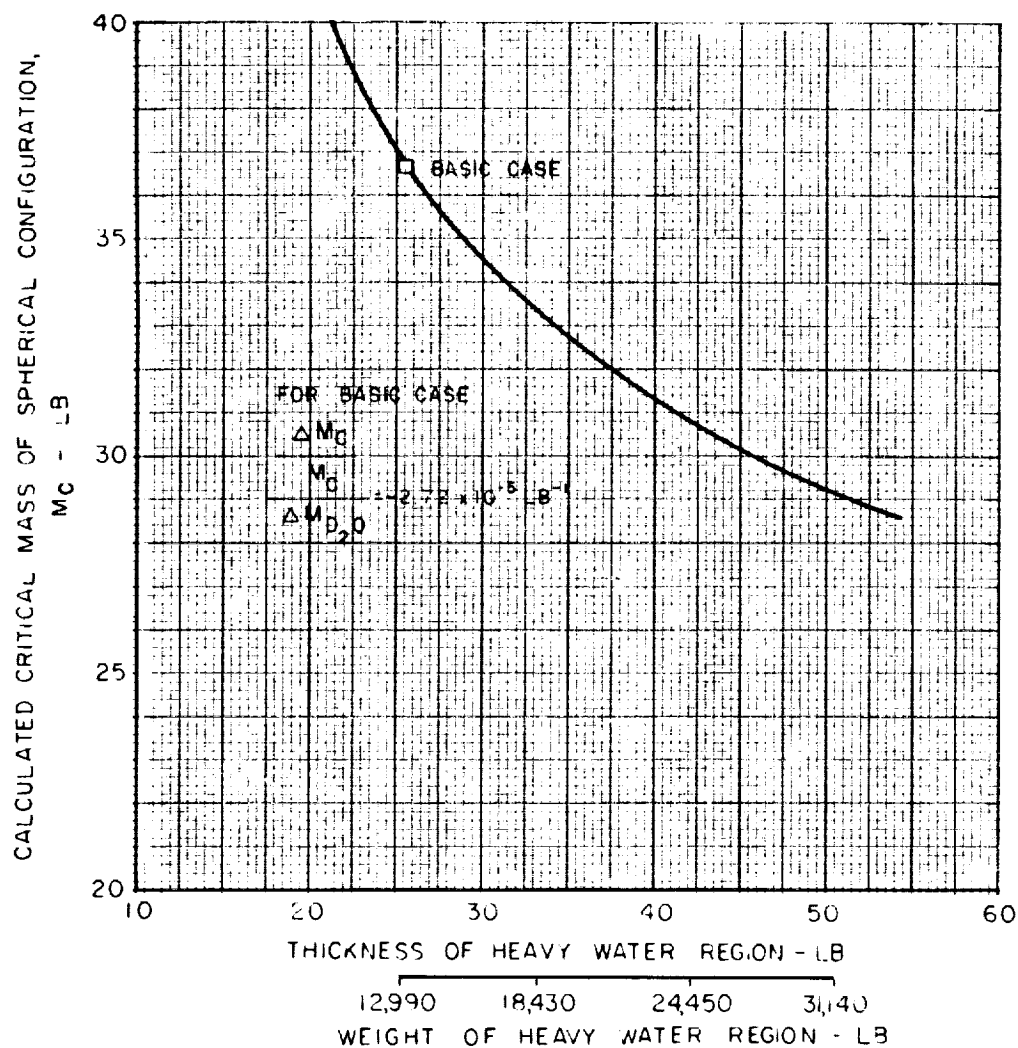
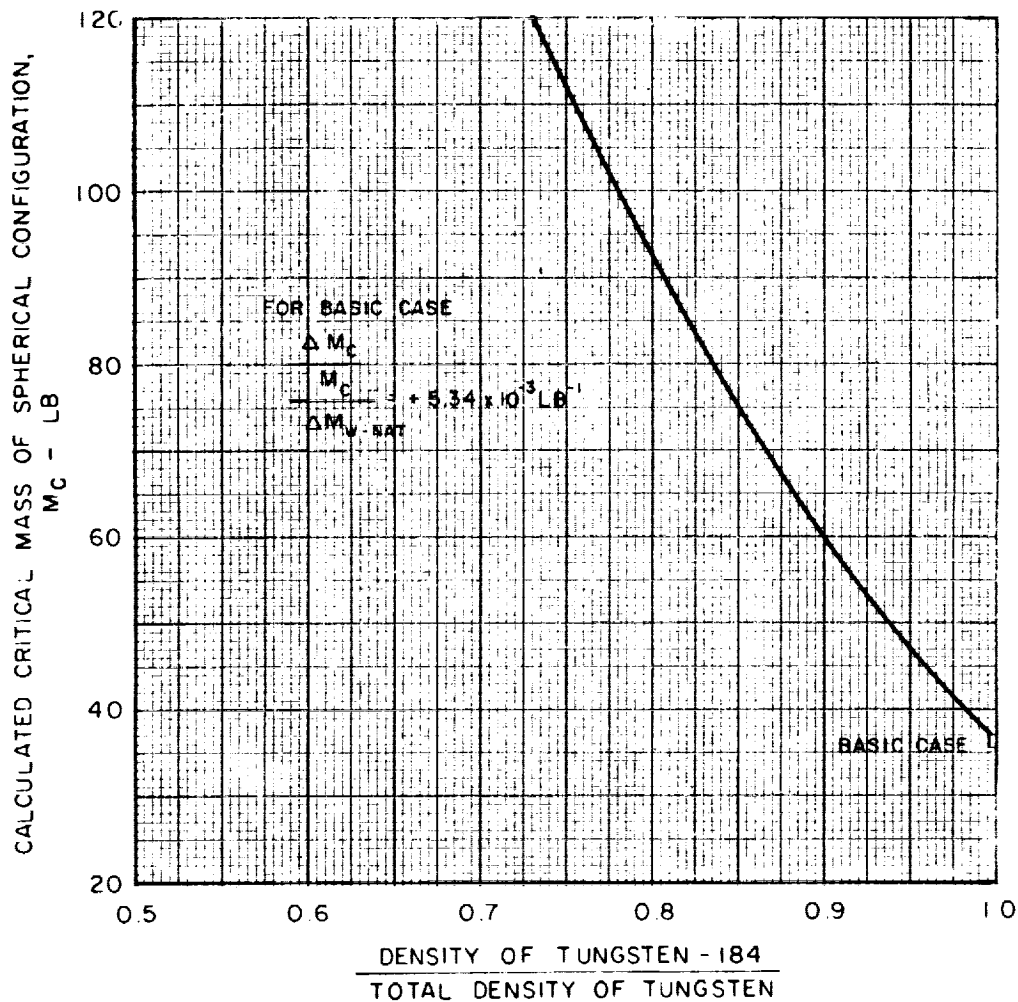


FIG. 20

ONE - DIMENSIONAL CALCULATION OF THE EFFECT OF VARIATION OF TUNGSTEN - 184 ENRICHMENT IN INNER LINER, BERYLLIUM OXIDE, GRAPHITE, AND HEAVY WATER REGIONS ON U-233 CRITICAL MASS

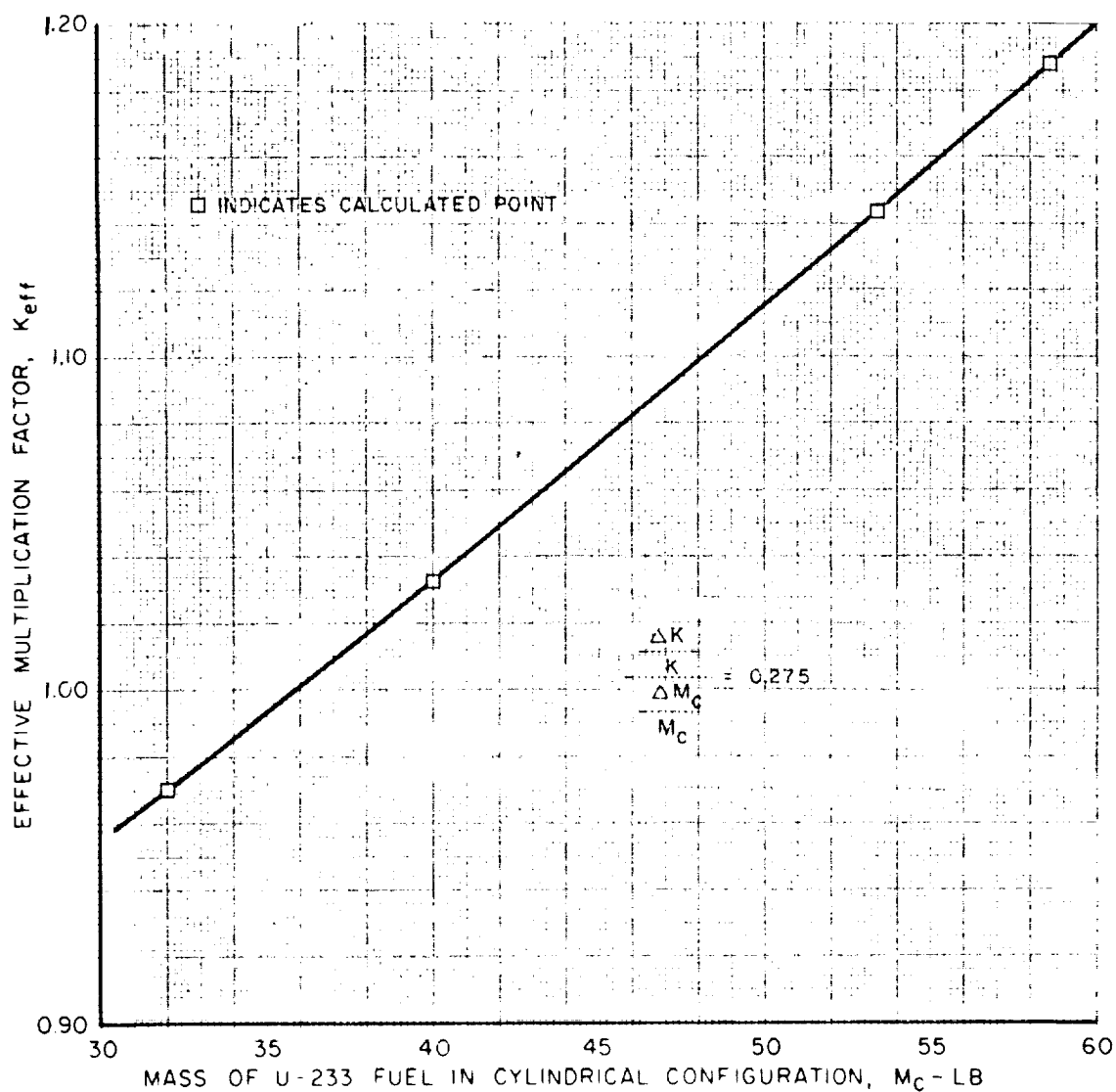
- CALCULATIONS MADE IN SPHERICAL GEOMETRY WITH UNIFORM FUEL DENSITY PROFILE
- ONE THERMAL NEUTRON ENERGY GROUP USED WITH AVERAGED CROSS SECTIONS FROM 24-NEUTRON-ENERGY-GROUP CALCULATIONS
- TOTAL WEIGHT OF TUNGSTEN IN INNER LINER AND MODERATOR REGIONS = 1218 LB



RESULTS OF TWO-DIMENSIONAL DIFFUSION THEORY CALCULATIONS FOR CYLINDRICAL CONFIGURATION WITH NO NOZZLES

- DIMENSIONS AND COMPOSITIONS USED IN CYLINDRICAL
CONFIGURATION GIVEN IN TABLES I AND II

- GEOMETRY FOR CYLINDRICAL CONFIGURATION
SHOWN IN FIG. 3



COMPARISON OF MID-PLANE RADIAL NEUTRON FLUX PLOTS FOR CYLINDRICAL CONFIGURATION WITH NO NOZZLE AND EQUIVALENT SPHERICAL CONFIGURATION

FLUXES NORMALIZED TO PEAK VALUE OF 1 NEUTRON/CM² - SEC

M_C - CYLINDER = 35.7 LB OF U-233

M_C - SPHERE = 55.1 LB OF U-233

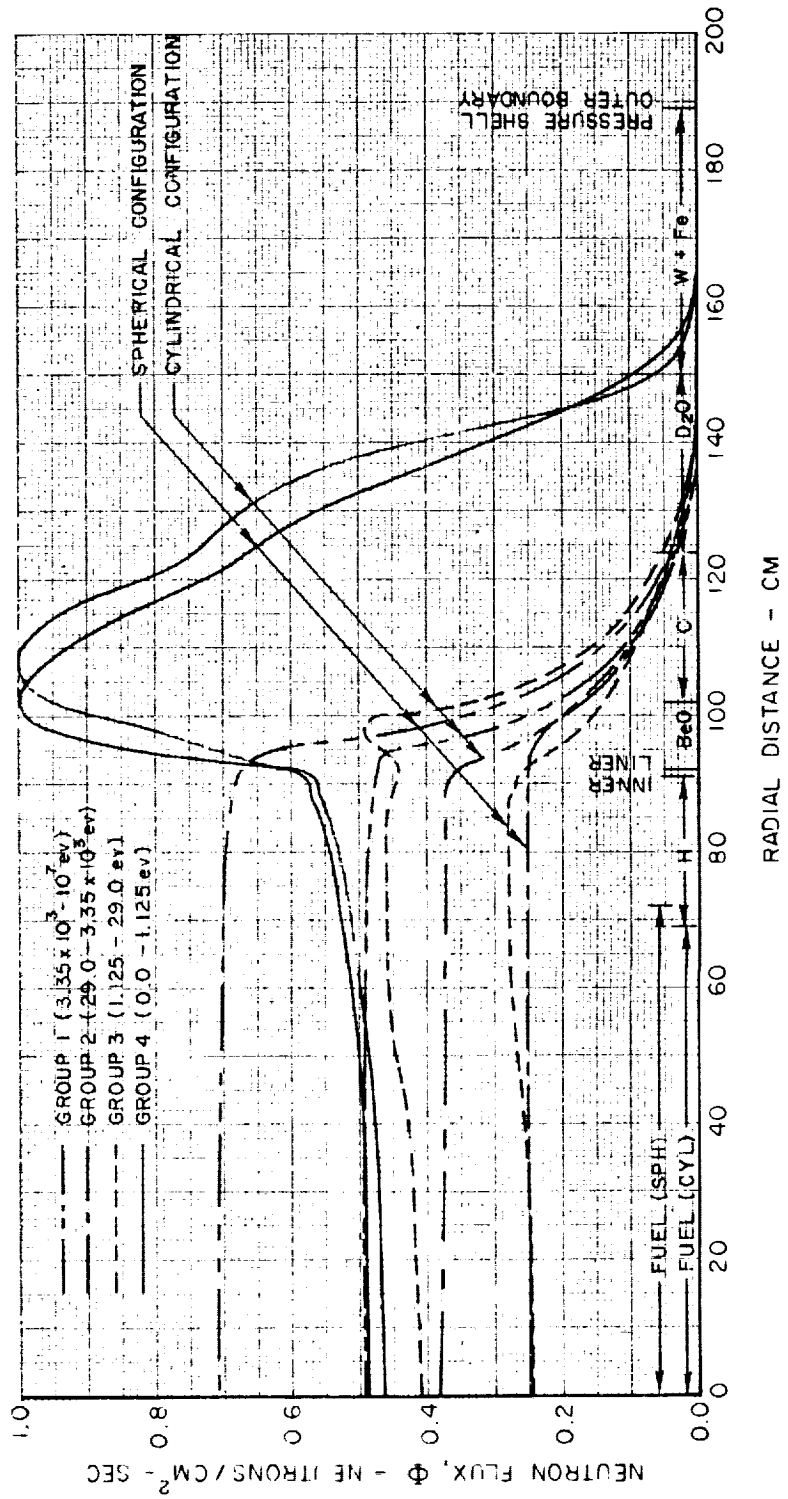


FIG. 22

CENTERLINE AXIAL NEUTRON FLUX PLOTS FOR CYLINDRICAL CONFIGURATION WITH NO NOZZLES

FLUXES NORMALIZED TO PEAK VALUE OF 1 NEUTRON/CM² - SEC

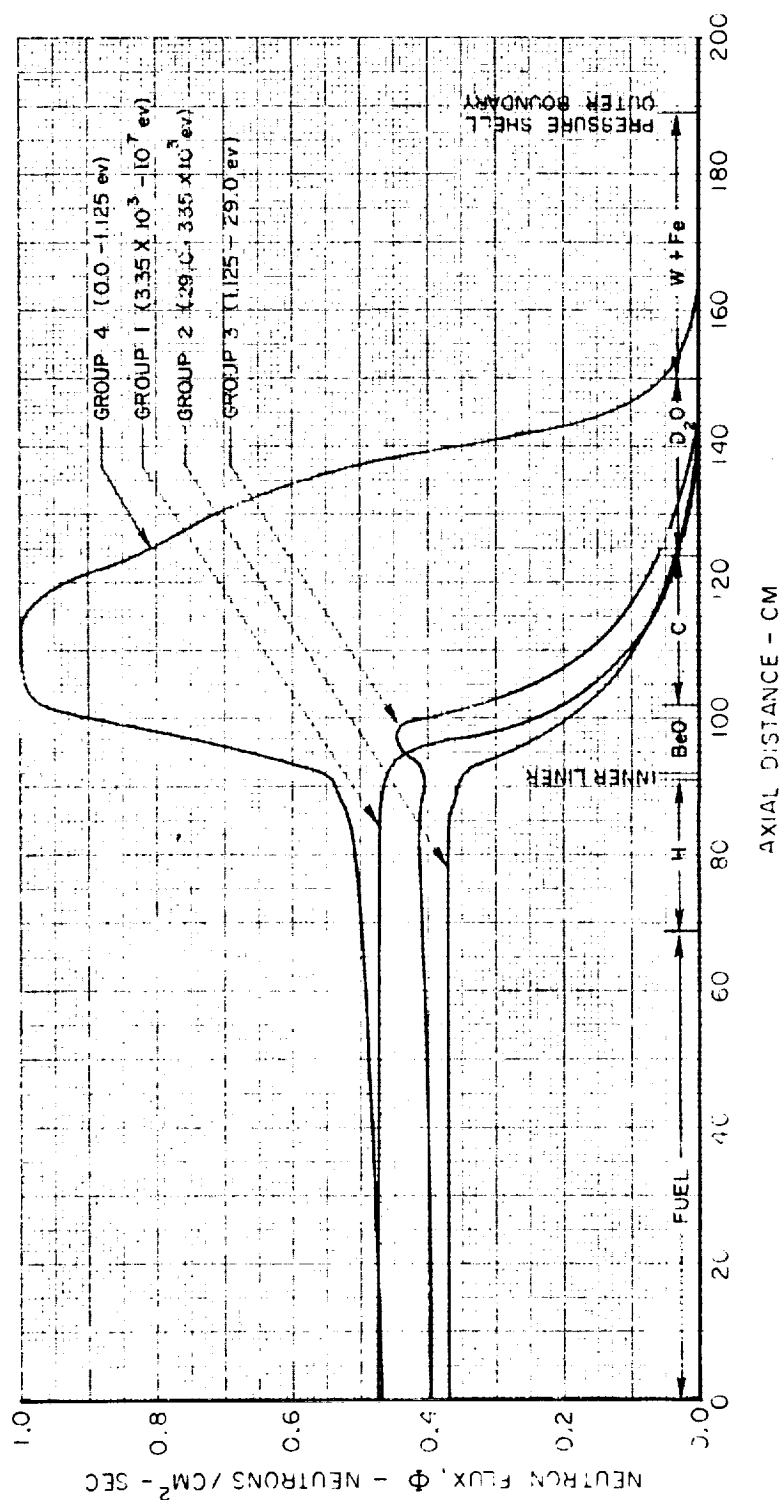


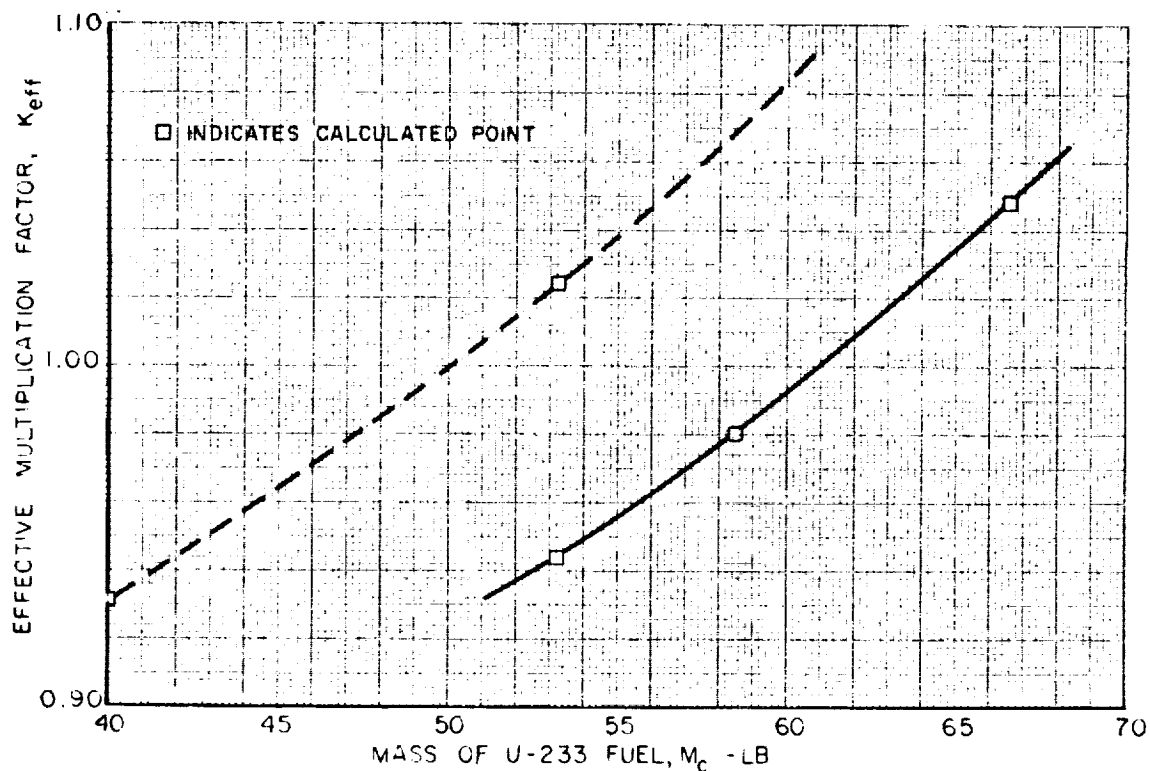
FIG. 23

RESULT OF TWO-DIMENSIONAL DIFFUSION THEORY CALCULATIONS FOR REFERENCE ENGINE DESIGNS WITH EXHAUST NOZZLE AND FUEL INJECTION DUCT

- GEOMETRY OF ENGINE NOZZLES AND FUEL INJECTION DUCT SHOWN IN FIGS 1,4 AND 5
- DIMENSIONS AND COMPOSITIONS FOR ALL REGIONS GIVEN IN TABLES III, IV AND V

TABLE OF RESULTS

LINE	CASE	M_c - LB	$\frac{\Delta K/K}{\Delta M_c/M_c}$
————	MODIFIED REFERENCE ENGINE DESIGN	60.9	0.487
-----	REFERENCE ENGINE DESIGN WITH NOZZLE APPROACH LINER SAME THICKNESS AS CAVITY INNER LINER	50.1	0.371



RADIAL NEUTRON FLUX PLOTS FOR MODIFIED REFERENCE ENGINE DESIGN THROUGH UPPER GRAPHITE MODERATOR REGION AND FUEL INJECTION DUCT

- FLUXES NORMALIZED SUCH THAT NEUTRON PRODUCTION IN FUEL REGION = 1 NEUTRON/SEC

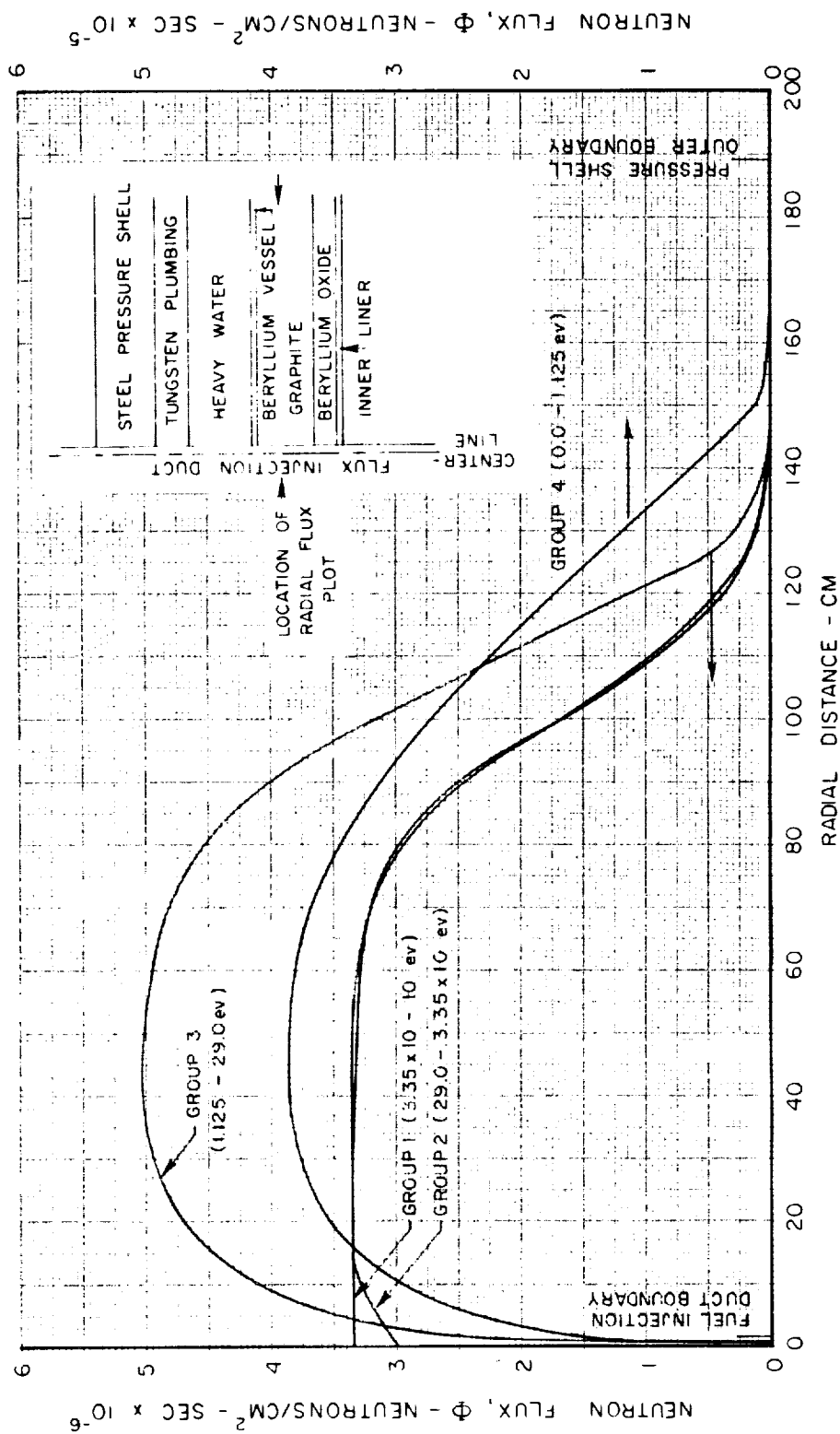


FIG. 25

MID-PLANE RADIAL NEUTRON FLUX PLOTS FOR MODIFIED REFERENCE ENGINE DESIGN

- FLUXES NORMALIZED SUCH THAT NEUTRON PRODUCTION IN FUEL REGION = 1 NEUTRON/SEC

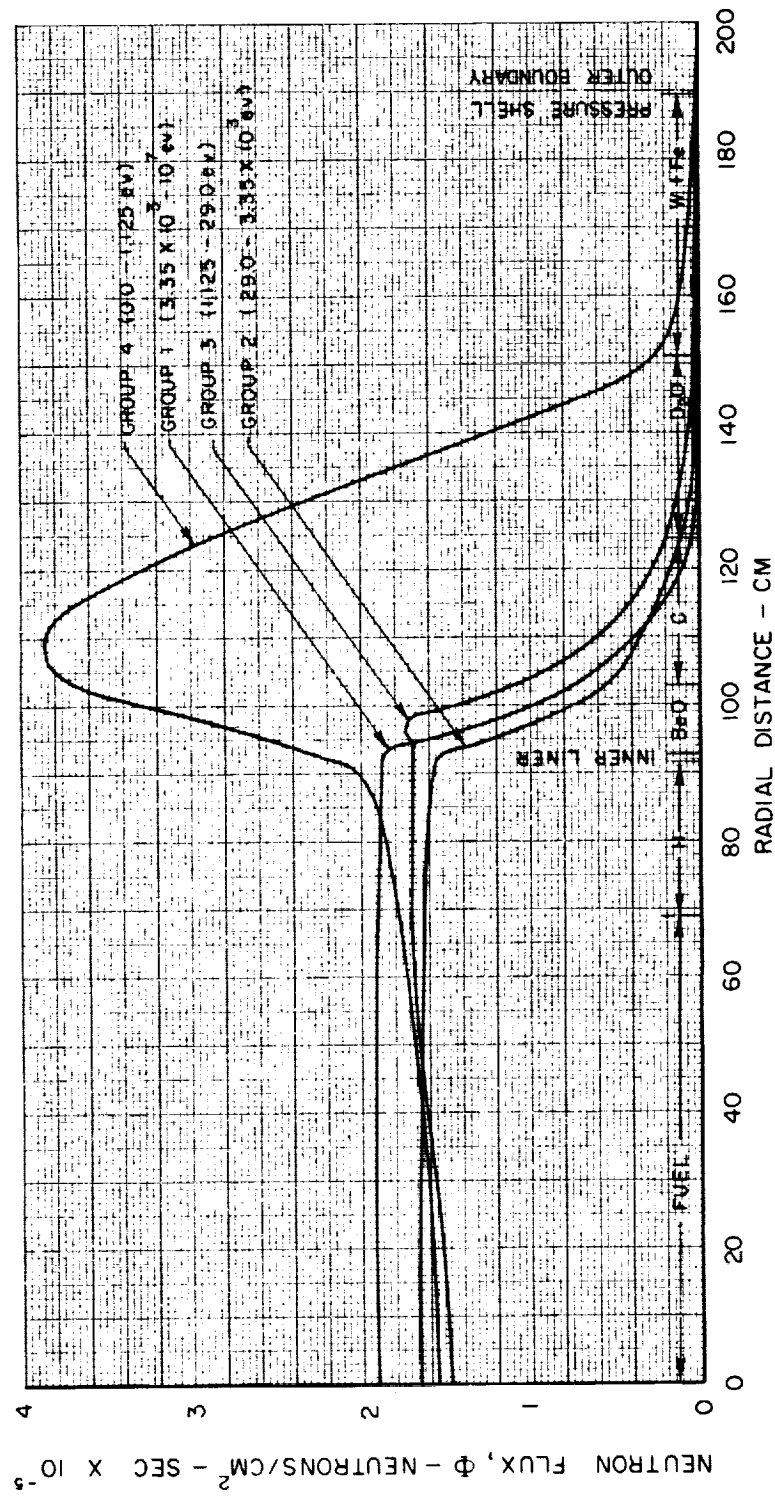


FIG. 26

RADIAL NEUTRON FLUX PLOTS FOR MODIFIED REFERENCE ENGINE DESIGN THROUGH AXIAL MID-PLANE OF NOZZLE APPROACH SLOT

- FLUXES NORMALIZED SUCH THAT NEUTRON PRODUCTION IN FUEL REGION = 1 NEUTRON / SEC

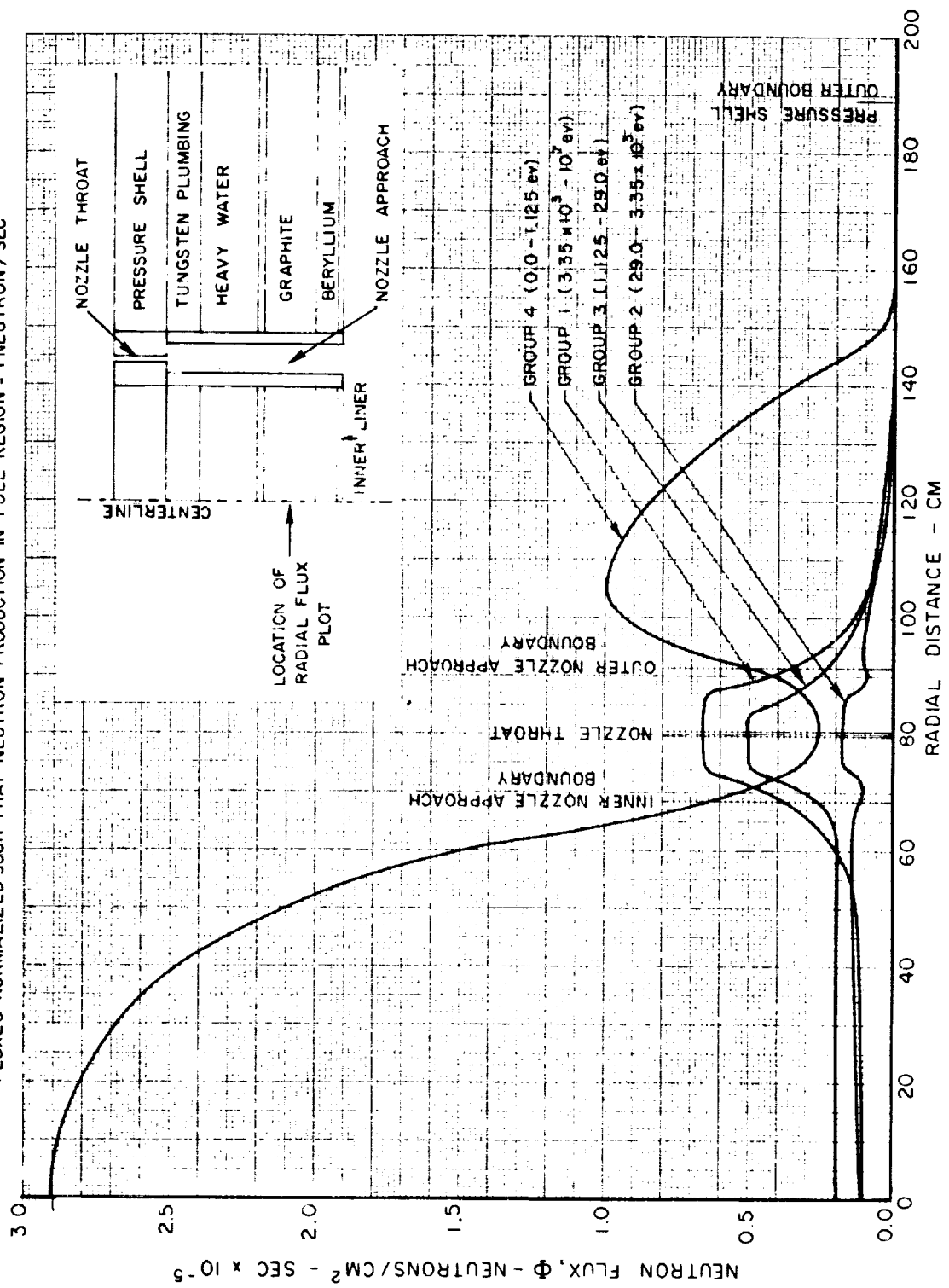


FIG. 27

RADIAL NEUTRON FLUX PLOTS FOR MODIFIED REFERENCE ENGINE DESIGN THROUGH AXIAL MID-PLANE OF NOZZLE THROAT

- FLUXES NORMALIZED SUCH THAT NEUTRON PRODUCTION IN FUEL REGION = 1 NEUTRON/SEC

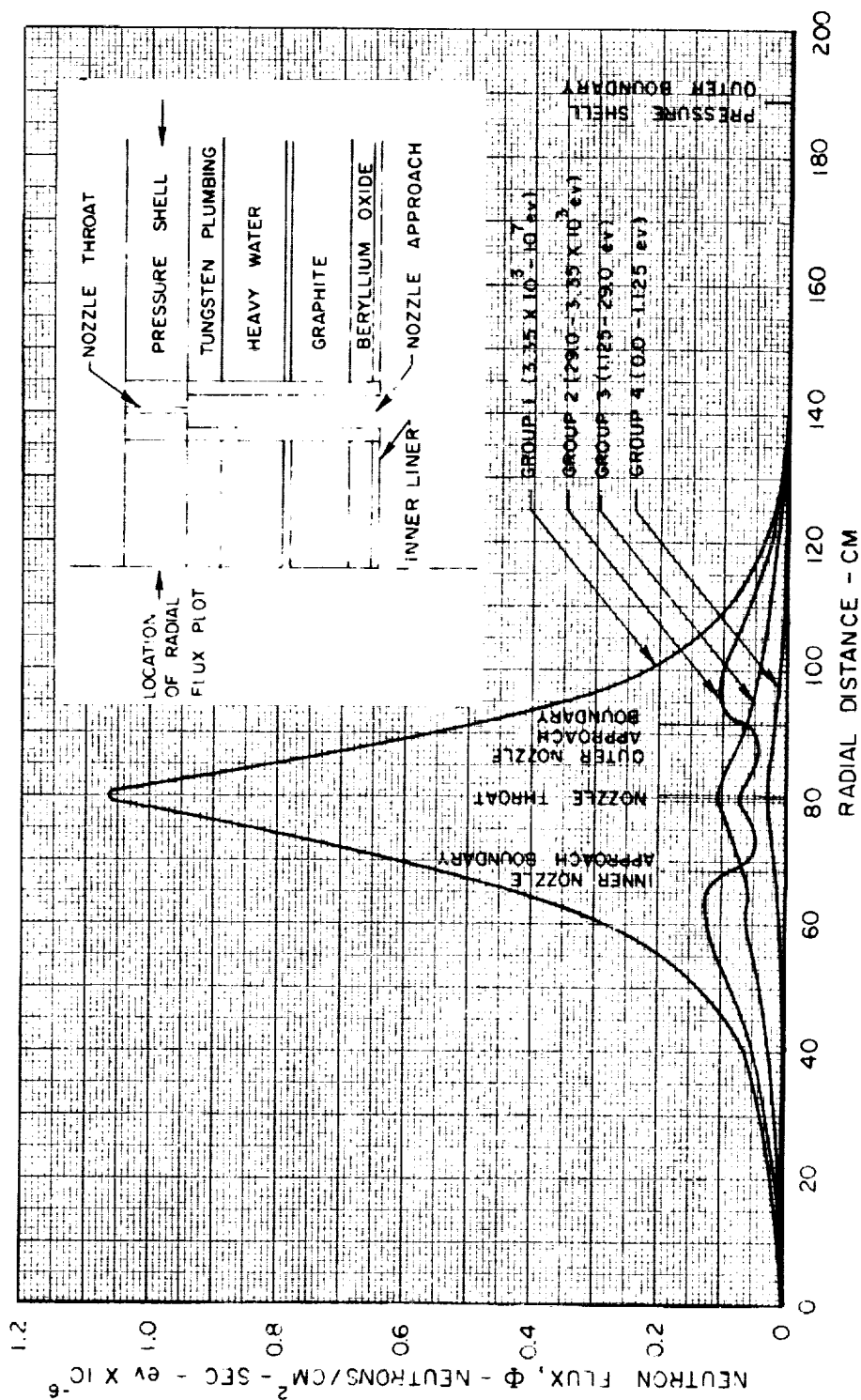


FIG. 28

03/11/2014

03/11/2014